Multiscale simulation of radiofrequency wave scattering in the scrape-off layer

Bodhi Biswas

York Plasma Institute, University of York. York, UK.

PPPL Theory Seminar. November 30, 2023.

This work is supported by the US DOE under grants DE-SC0018090, DE-SC0014264, and DE-FC02-04ER54698.

Scattering is a problem for RF-driven heating and current drive actuators in tokamaks

Objective: localised resonant power deposition
- Increase fusion output
- Non-inductive operation
- Shape q-profile
- Suppress NTMs

Scattering modifies wave-spectrum, leading to:
- Decreased antenna-core coupling.
- Broadening and displacement of power deposition peak.
- Introduces large uncertainties in predictive models.

Lower hybrid current drive (LHCD) is sensitive to wave-trajectory

- Lower hybrid (LH) waves ($\Omega_i^2 \ll \omega^2 \ll \Omega_e^2$) efficiently drive current by electron Landau damping.
- Strong linear electron Landau damping (ELD) condition: $N_{||} \equiv \frac{k_{||}c}{\omega} \gtrsim \frac{c}{3v_{te}}$
- $N_{||}$ evolves along the wave-trajectory. CD performance can be sensitive to initial launch and plasma parameters.

Theoretical model for LHCD:

Wave propagation — Ray-tracing (i.e. GENRAY)

Wave damping

Modification of $f_e(\boldsymbol{v})$

Fokker-Planck solver (i.e. CQL3D)

Calculate current: $j_{||} = -e\int v_{||} f_e(v_{||}) dv$

Multi-pass regime in Alcator C-Mod

If $N_{||0} < \frac{c}{3v_{te}}$ $\rightarrow$ long wave trajectories.

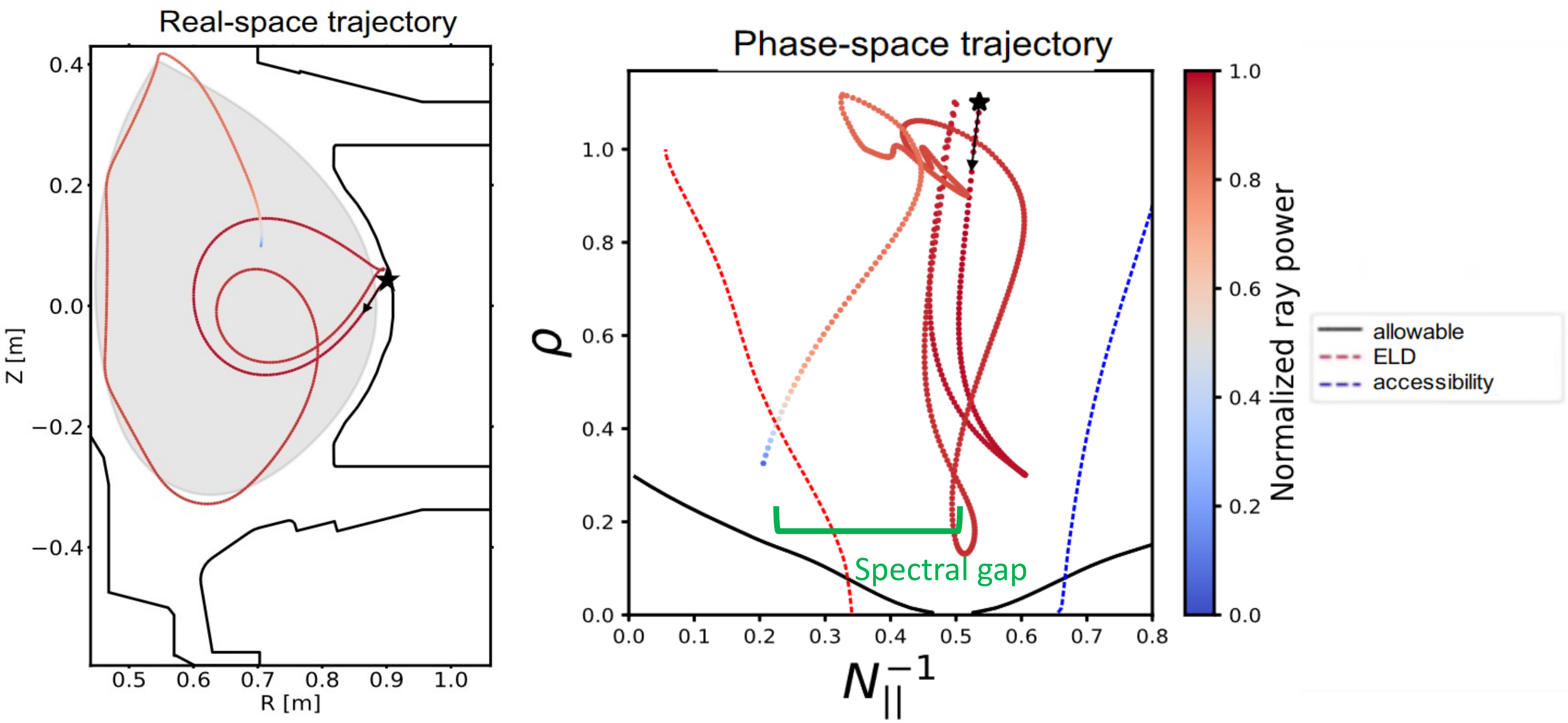

The multi-pass regime is notoriously difficult to model

- The *spectral-gap problem*: $\left|N_{||_0}\right| < \frac{c}{3v_{te}}$
- Standard Ray-tracing/Fokker-Planck simulations cannot resolve the spectral gap.
  - Inaccurate
  - Not robust
- LH waves must propagate through the highly turbulence SOL region. Direct experimental evidence of scattering[1].
- **How does scattering affect the wave-spectrum? Can it explain measurements in Alcator C-Mod?**

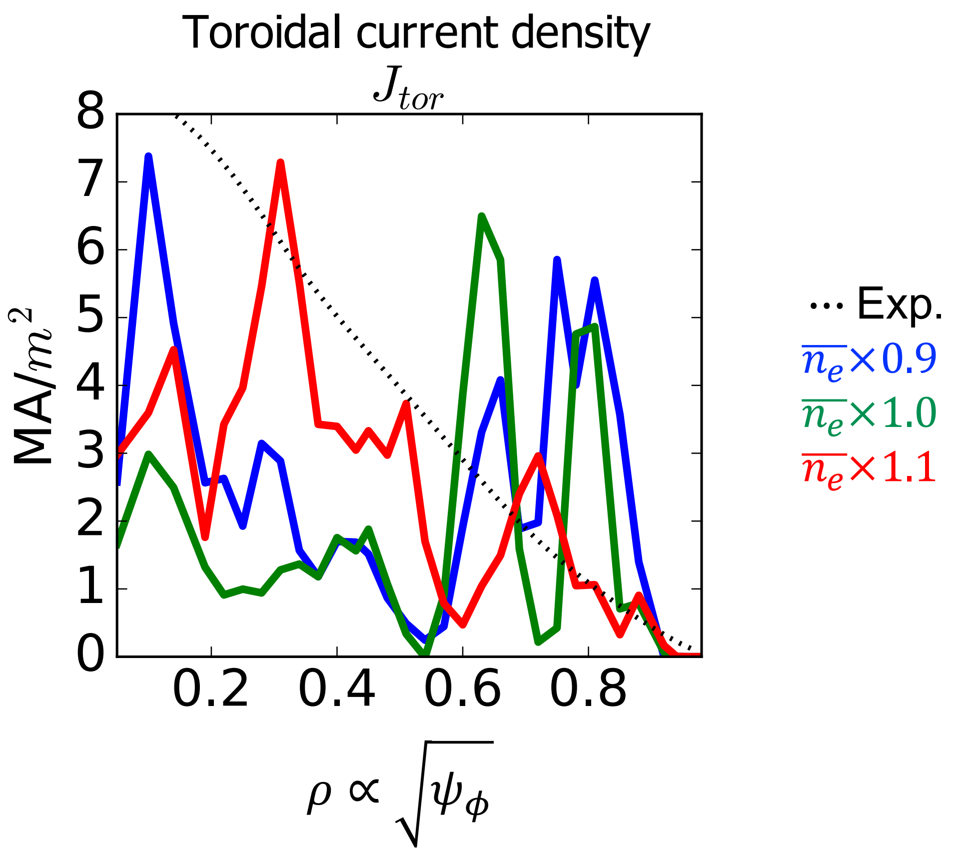

C-Mod fully non-inductive plasma

[1]Martin et al., NF. 2019.

Nature of edge turbulence and scattering

- Turbulence is largely field-aligned ($\nabla_{||} n \sim 0$)
- RF scattering rotates $k_\perp$, and breaks toroidal mode-number ($\mathcal{N} \equiv k_\phi R$) conservation.

- Filaments are dense and spatially localized[1,2]

$$n_b/n_0 \approx 1 - 10$$
$$a_b \approx 0.5 - 5 \text{ cm} \sim 1/k_\perp$$
$$k_\perp L_n \sim 1$$

- Highly intermittent[2,3]
- Strongest at outer mid-plane[4]

- Ad-hoc introduction of $k_\perp$ angle rotation can reproduce LHCD measurements in C-Mod.[5] **Could edge turbulence account for this?**

Gas puff imaging (GPI) in C-Mod

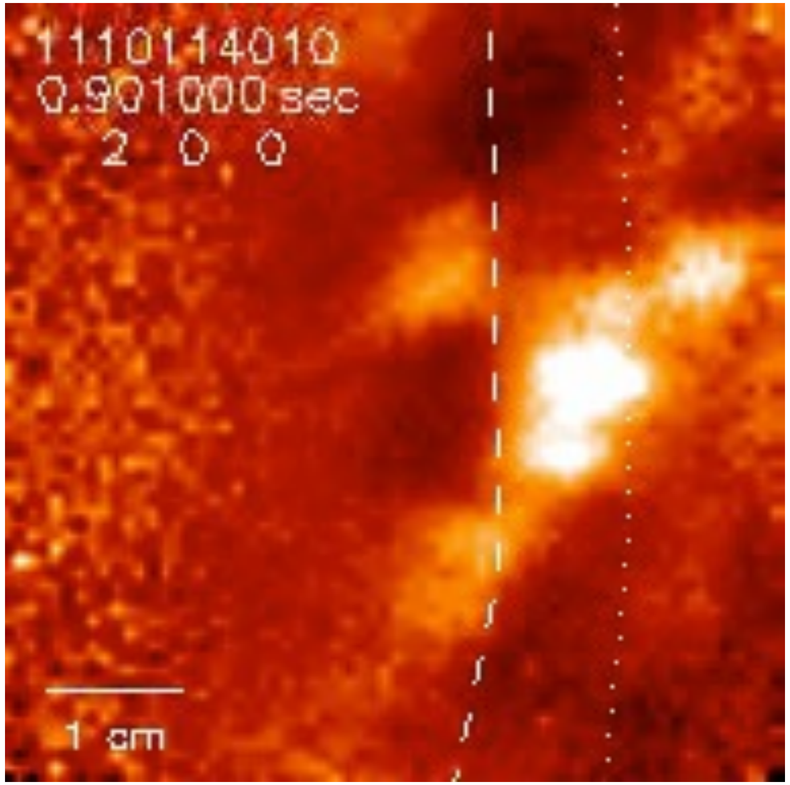

S Zweben, PPPL.

[1]Zweben et al., PPCF. 2016.
[2]Zweben et al., PoP. 2002.
[3]Kube et al., PPCF. 2016.
[4]Terry et al., PoP. 2003.
[5]Baek et al., NF. 2021.

Spatial coherency and intermittency of turbulence impacts wave-scattering

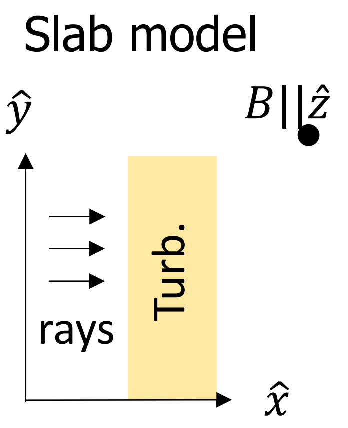

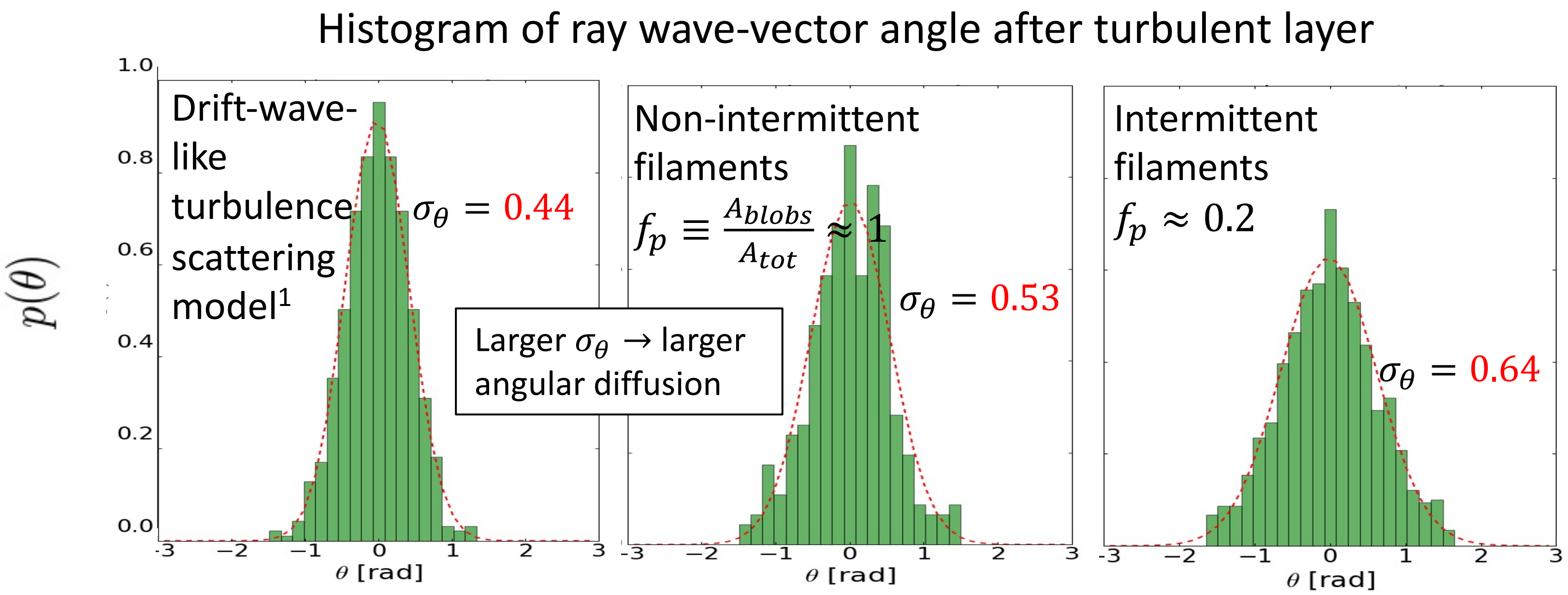

$\theta \equiv sin^{-1}(k_y/k_x)$.

Previous drift-wave-like models under-predict scattering.[2]

[1]Bonoli and Ott, PoF. 1982.
[2]Biswas et al., PPCF. 2020.

Hierarchy of RF wave scattering models

Increasing fidelity and computational cost →

Reduced ray-tracing models		

Drift-wave turbulence
- Ray-tracing (diffusive broadening of $\boldsymbol{k}_\perp$) [1]
- Wave-kinetic approach [2,3]

Fast solve

SOL turbulence is filamentary

Filamentary turbulence
- Ray-tracing over synthetic turbulence [4]
- Limited validity ($k_\perp L_n \sim 1$)

Increased accuracy

Limited validity

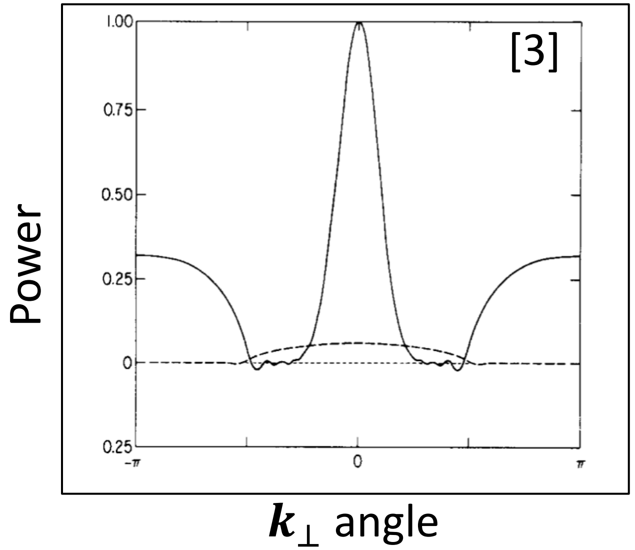

[1] Bellan and Wong, PoF. 1978.
[2] Bonoli and Ott, PoF. 1982.
[3] Andrews and Perkins, PoF. 1983.
[4] Biswas et al., PPCF. 2020.

[4]

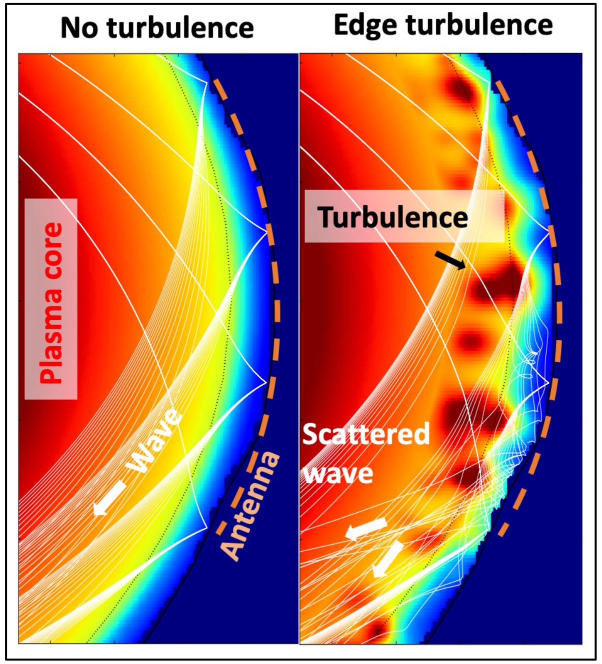

Hierarchy of RF wave scattering models

Increasing fidelity and computational cost

		Full-wave models

Single wave-filament interaction

- Analytic solution available [1,2]

Fast solve

Only one filament

Multiple filaments or whole SOL

- Numeric full-wave solvers [3,4]

All optical effects

Computationally expensive

Coupling to core solver is non-trivial

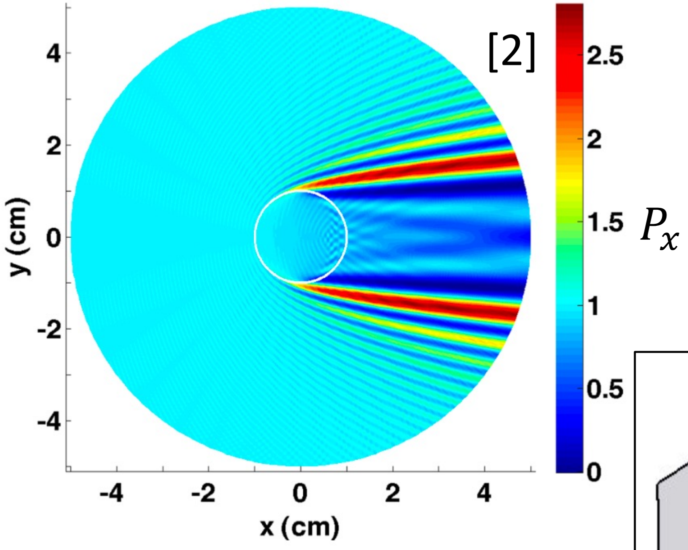

[1] Myra and D'Ippolito, PoP. 2010.
[2] Ram and Hizanidis, PoP. 2016.
[3] Shiraiwa et al., EPJ Web of Conf. 2017.
[4] Lau et al., NF. 2020.

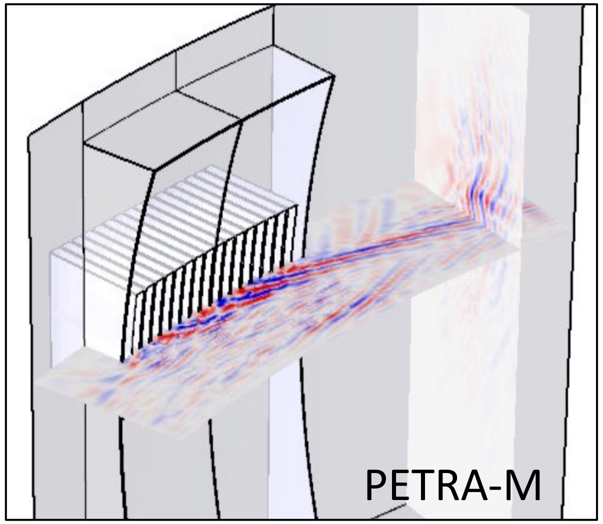

Hierarchy of RF wave scattering models

Increasing fidelity and computational cost

	Multiscale full-wave/ray-tracing solver	

At wave-filament interaction:
$k_\perp L_n \sim 1.$ **Apply full-wave solver**
Elsewhere:
$k_\perp L_n \gg 1.$ **Ray-tracing is acceptable**

Couple using radiative transfer theory

Fast solve
Many optical effects
Straightforward coupling to core solver

Single filament full-wave…

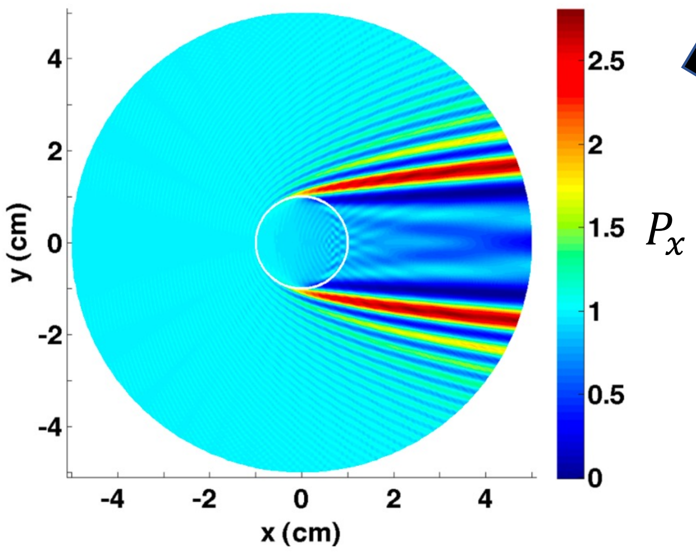

… coupled to ray-tracer.

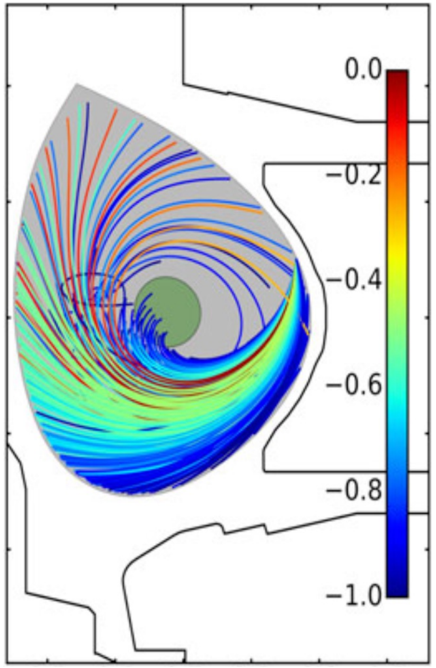

A single wave-filament interaction

- Plane wave interacting with a field-aligned, infinitely long, cylindrical filament.
- Poloidally symmetric.
- Analytic, series solution to scattered waves (slow and fast branch).

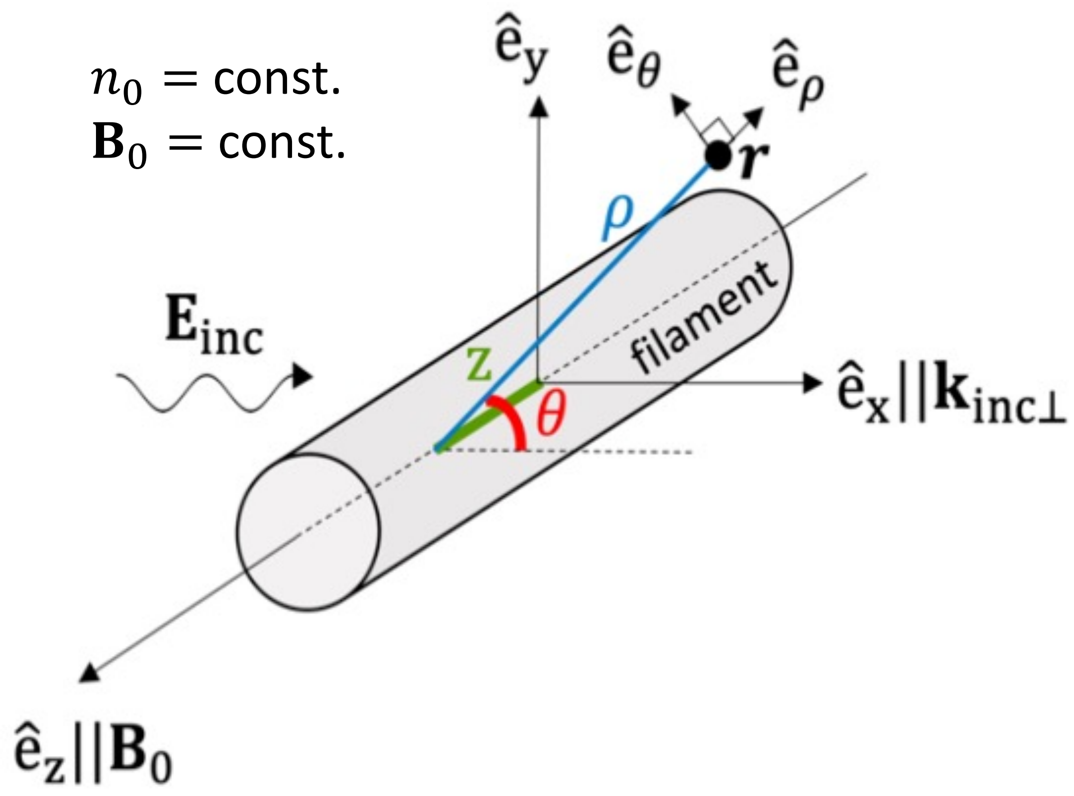

Solution scheme for a radially tapered filament

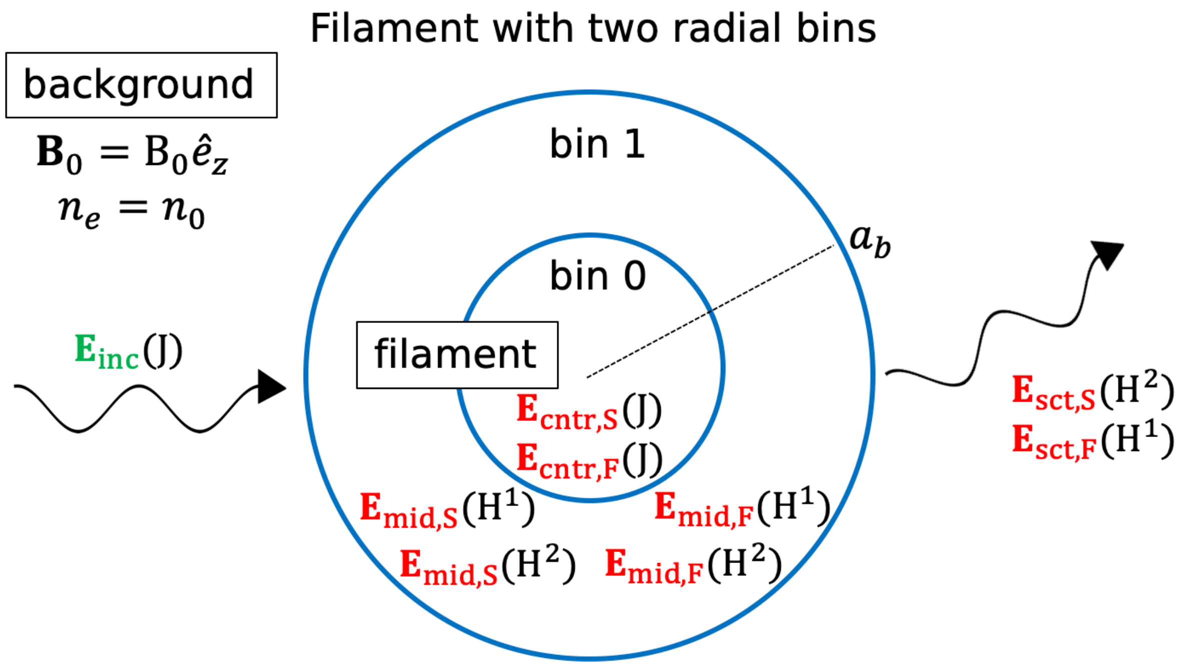

Vector Helmholtz equation solved by separation of variables.

Known: Bessel coefficients for incident Lower Hybrid slow wave.

Unknown: Bessel coefficients for slow and fast waves, both inside and outside filament.

Boundary conditions: Maxwell BC's at the edge of each radial bin.

Leads to linear system of equations with unique solution. Very fast solve!

Calculating scattering-width

Case setup:
4.6GHz Slow wave launched in +x direction.
$N_{||} = 2$
$B = 4\text{T}$

→ *Compute electric field* → *Compute Poynting flux* → *Compute scattering-width*

Gaussian filament with half-max full-width size:
$a_b = 0.5cm.$

Filament density

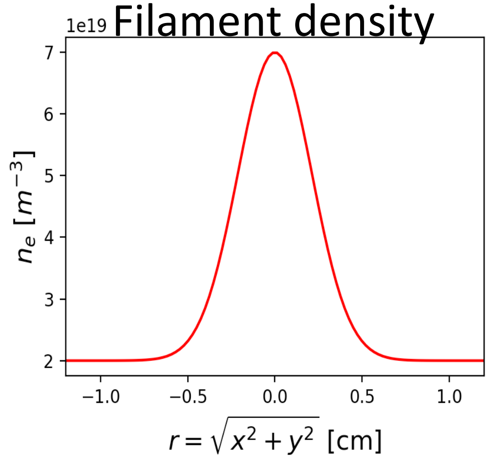

Normalized electric field

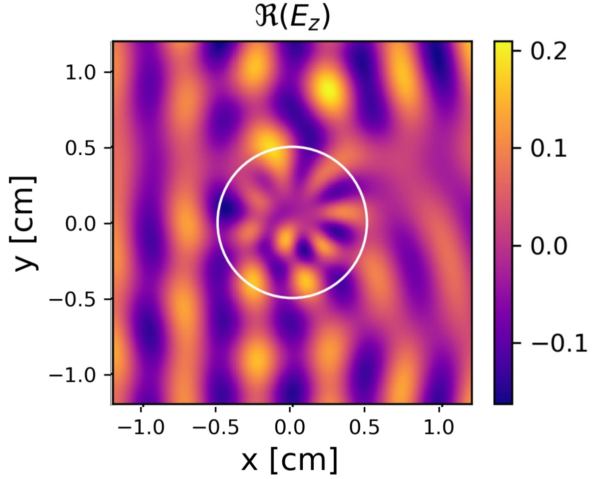

Normalized Poynting flux

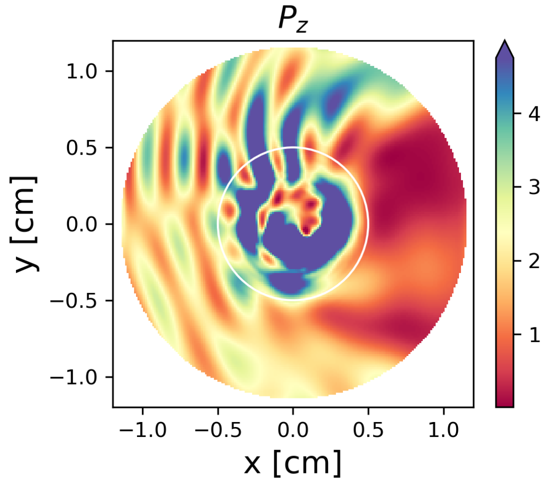

Normalized differential scattering-width for S→S (like-mode) scattering

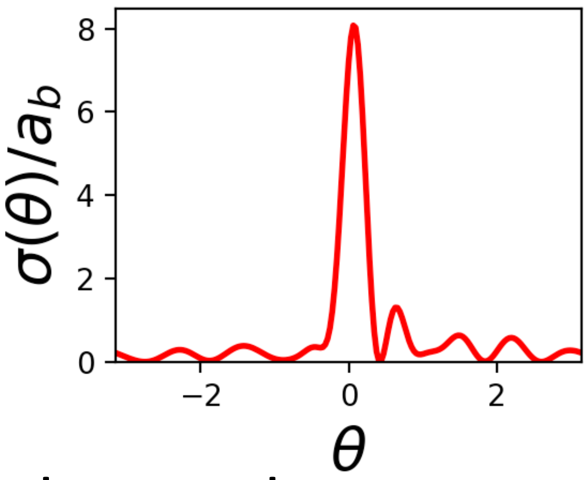

Validated against numeric finite-element wave-solver PETRA-M[1]. Excellent agreement.

[1]Shiraiwa et al., EPJ Web Conf. 2017.

Parametric scan of filament parameters

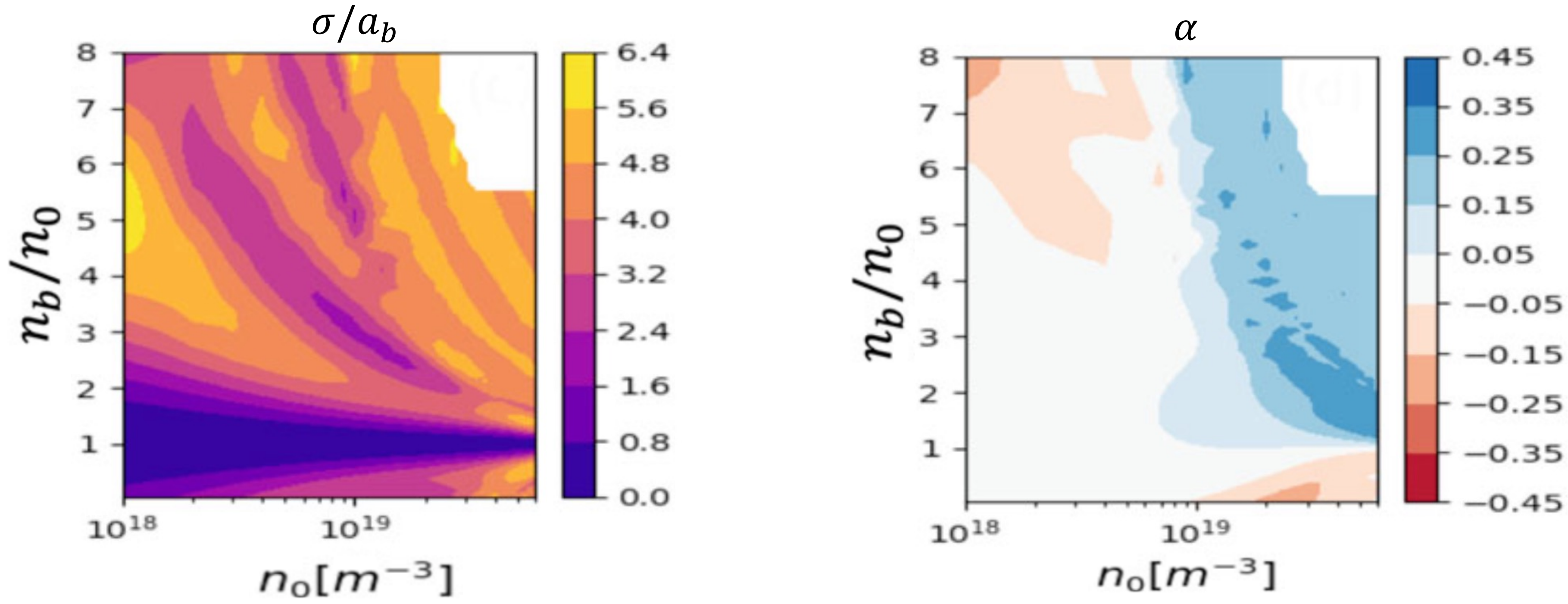

$$\alpha = \frac{\int_0^{\pi} \sigma(\theta)d\theta}{\int_{-\pi}^{\pi} \sigma(\theta)d\theta} - \frac{1}{2}$$

so that

$\alpha > 0 \rightarrow$ net +y scatter
$\alpha < 0 \rightarrow$ net -y scatter

4.6GHz slow-wave launched at $N_{||} = 2$.
$a_b = 0.85$cm

Asymmetric scattering not captured in ray-tracing

WKB validity for LH waves: $\frac{|\epsilon_{xy}|}{k_\perp L_n} \ll 1$

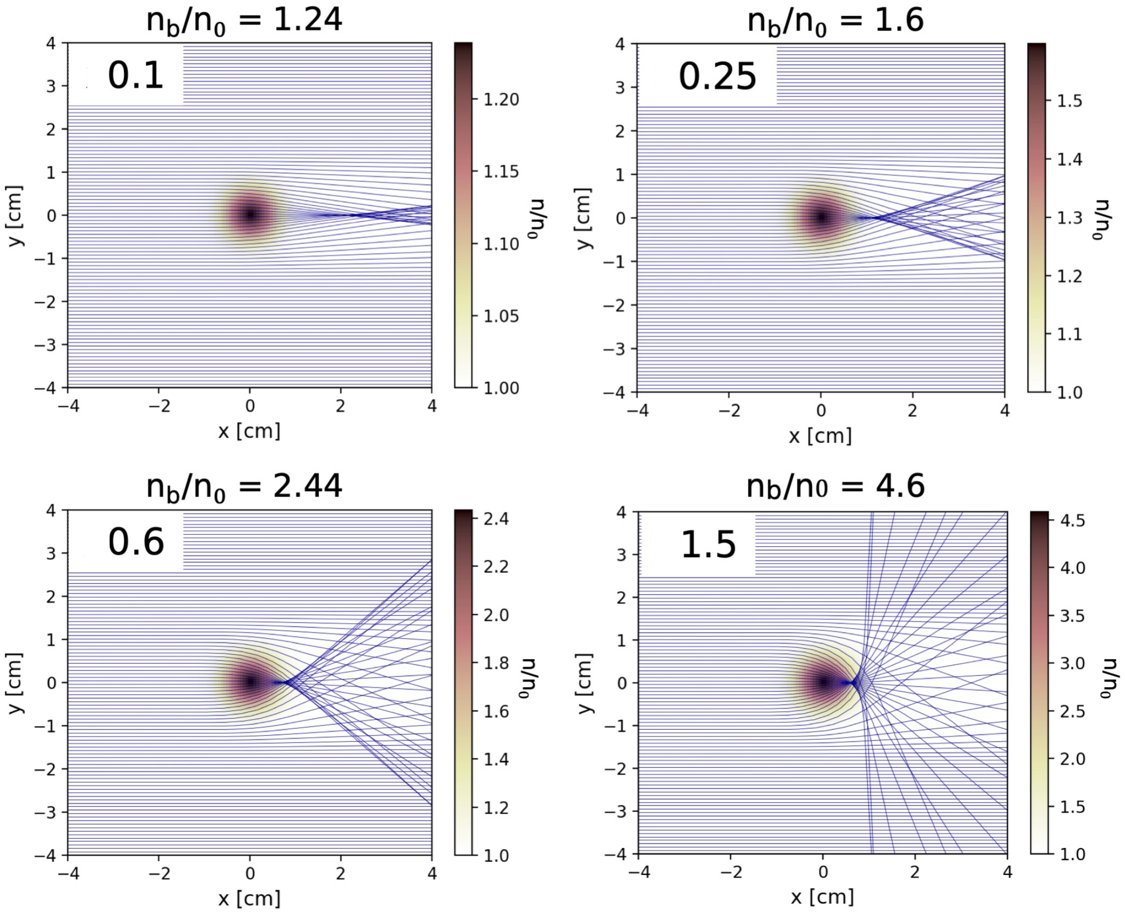

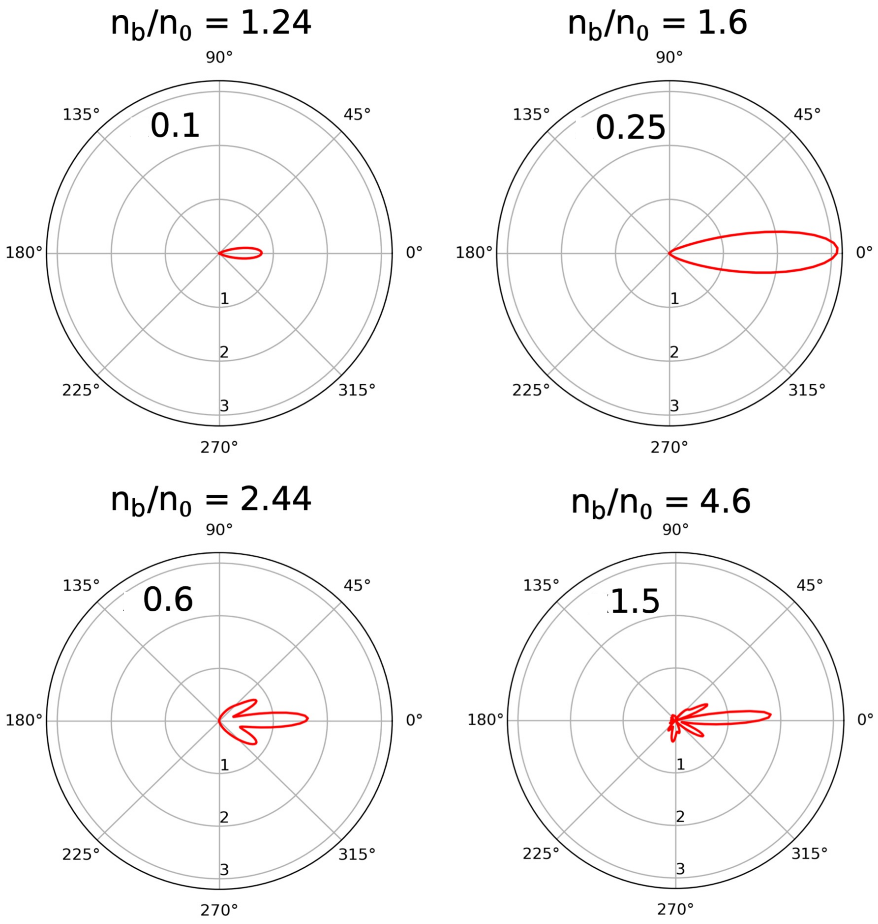

Symmetry broken by orientation of magnetic field. This is a higher-order (full-wave) effect.

Averaging over filament statistics

$$\sigma_{\mathrm{eff},j\to j'}(\theta) = \int_0^\infty \mathrm{d}a_b \int_0^\infty \mathrm{d}\,(n_b/n_0)\; \sigma_{j\to j'}(\theta; n_b/n_0, a_b)\, p(n_b/n_0, a_b) \quad \text{[units: L]}$$

Differential scattering-width

Filament probability distribution function (PDF)

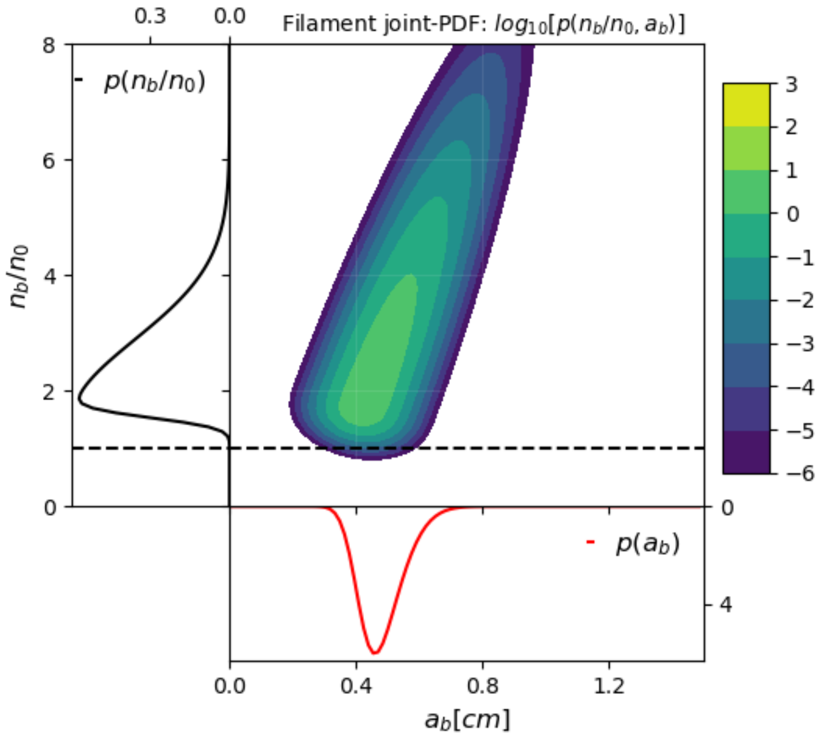

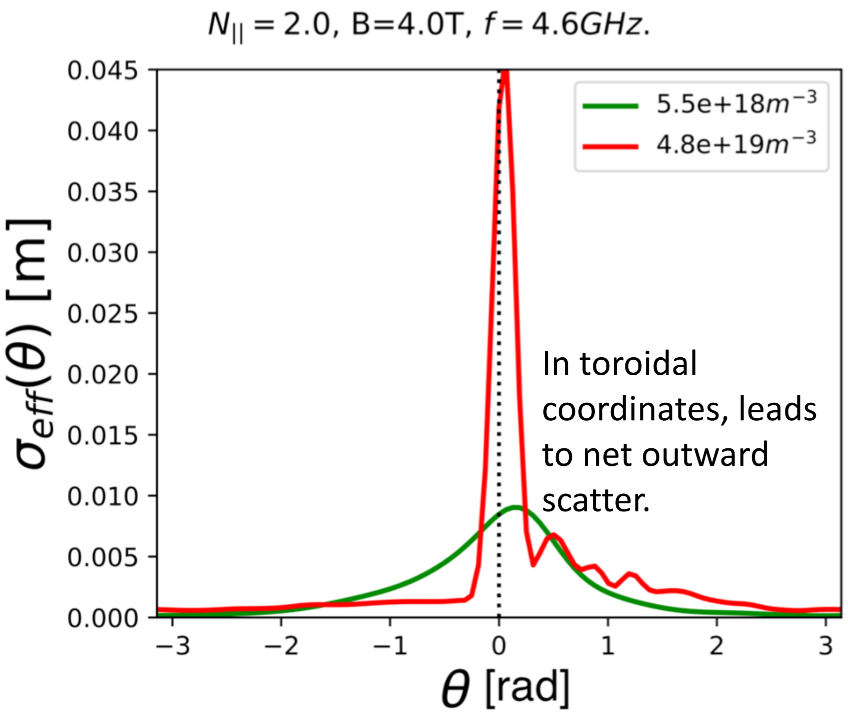

In toroidal coordinates, leads to net outward scatter.

Multiple scattering events modeled with radiative transfer equation (RTE)

Σ_{eff} is the inverse mean free-path for a wave-packet to scatter with a filament.

packing-fraction

$$\Sigma_{\text{eff}} = \frac{f_p}{\pi \langle a_b \rangle^2} \sigma_{\text{eff}}$$

average filament size

This can be used to formulate the RTE

$$\left(\frac{dP_j}{dt}\right)_r + 2\gamma(\mathbf{k}_j, \mathbf{r}) P_j = \left(\frac{dP_j}{dt}\right)_{\text{sct}} \qquad j = S, F$$

Out-scatter

$$\hat{\sigma}(\theta) \equiv \sigma(\theta)/\sigma$$

In-scatter

$$\left(\frac{dP_j}{dt}\right)_{\text{sct}} = \sum_{j'=S,F} -\Sigma_{\text{eff},j\to j'}(k_{||}, \mathbf{r}) |\mathbf{v}_{gr\perp}(\mathbf{k}_j, \mathbf{r})| P_j$$
$$+ \sum_{j'=S,F} \Sigma_{\text{eff},j'\to j}(k'_{||}, \mathbf{r}) |\mathbf{v}_{gr\perp}(\mathbf{k}_{j'}, \mathbf{r})| \int_{-\pi}^{\pi} \hat{\sigma}_{\text{eff},j'\to j}(\theta - \theta'; k_{||}, \mathbf{r}) P_{j'}(\theta', k_{||}, \mathbf{r}) d\theta'$$

First, a simple slab problem

Assumptions:

- Turbulent layer of width L_x
- homogenous background and turbulence parameters
- initial slow wave at normal incidence
- neglect possibility of mode-conversion to fast wave

OK approximation for scatter in front of LH grill.

In-scatter

$$cos\theta \frac{dP(x,\theta)}{dx} = -\Sigma_{\text{eff}} P(x,\theta) + \Sigma_{\text{eff}} \int_{-\pi}^{\pi} \hat{\sigma}_{\text{eff}}(\theta - \theta') P(x,\theta') d\theta'$$

Out-scatter

This equation can be solved by a Markov Chain.
See Biswas et al., JPP. 2021.

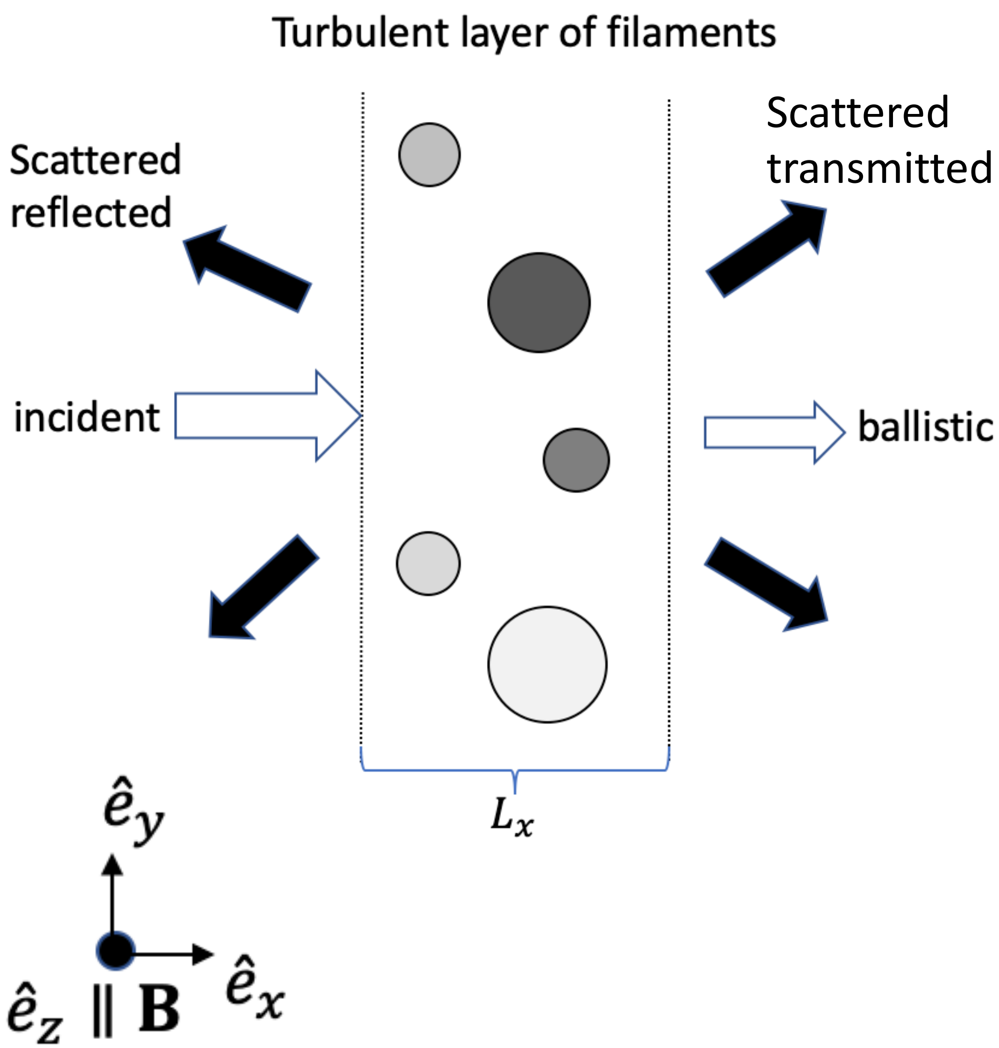

Solving RTE in slab geometry using an absorbing Markov chain

Similarities with radiation modeling in atmospheric science[1].
Discretize turbulent layer width $x = [0, L_x]$ and angle of photon trajectory $\theta = [-\pi, \pi]$.

Transmitted wave-spectrum:

$$\mathrm{P_T}(\theta_{n'}) \approx \mathbf{\Pi} \cdot (\mathbf{I} - \mathbf{T})^{-1} \cdot \mathbf{R}_\mathrm{T}$$

Source of incident photons at (x_i, θ_l)

Probability to **transition** from $(x_j, \theta_m) \rightarrow (x_{j'}, \theta_{m'})$

Probability to **escape** via transmittance from $(x_k, \theta_n) \rightarrow (L_x, \theta_{n'})$

Fast, deterministic method to solve the RTE.

[1]*Esposito et al., The Astrophysical Journal. 1978.*

Markov Chain (MC) used to model LH scattering in front of antenna

Inputs:

$\sigma_{eff}(\theta)$

f_p

$L_x = 2.5$ cm

MC

Outputs:

$P_{sct}(\theta)$: angle-broadened wave-spectrum

F_{bal}: fraction of ballistic power.

F_T: fraction of non-ballistic transmitted power.

F_R: fraction of reflected power.

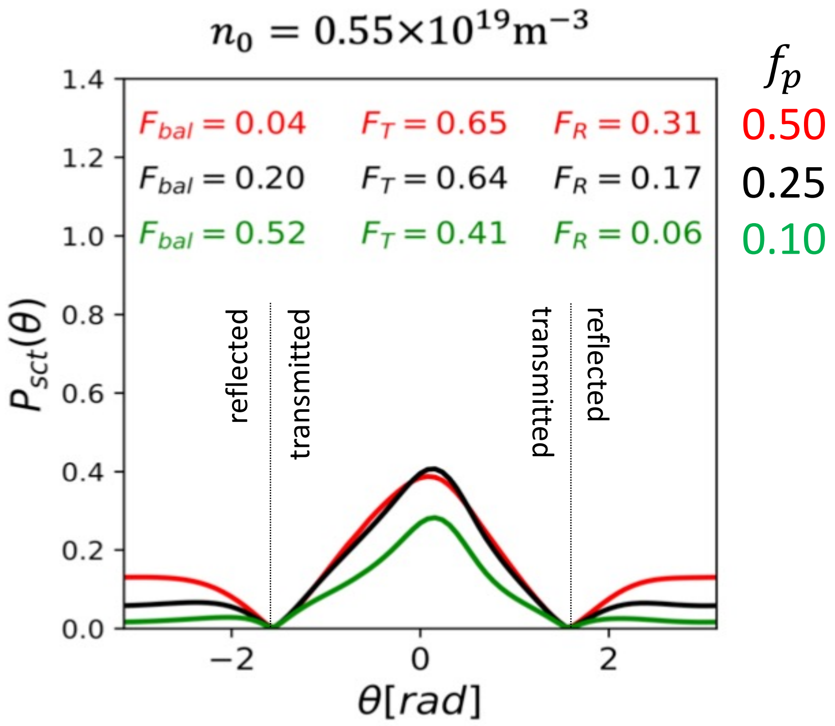

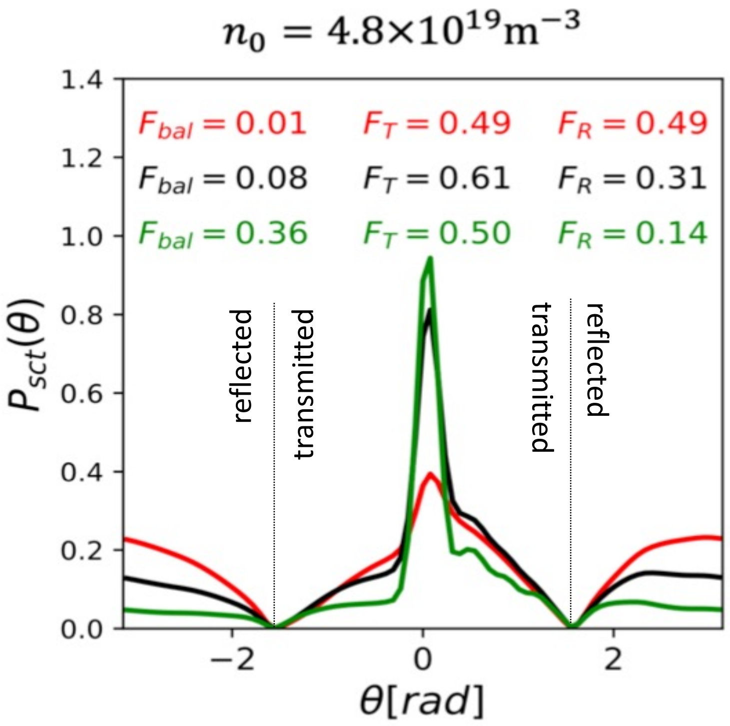

Model comparison against Petra-M

Simulation setup in finite-element code PETRA-M.

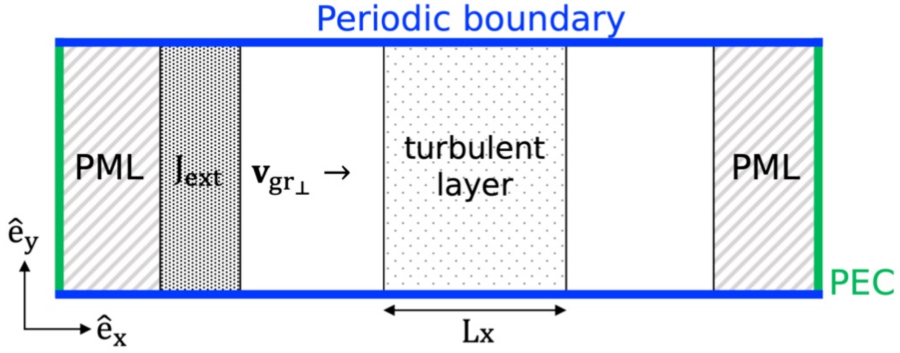

Case #	Plasma parameters					$\Sigma_{eff}L_x$	F_{ref}	
	$n_0 \times 10^{19}$ [m^{-3}]	$\langle n_b/n_0 \rangle$	$\langle a_b \rangle$ [cm]	f_p	L_x [cm]		Petra-M	Multiscale
1	0.55	2.60	0.48	0.02	5.0	0.26	0.01	0.02
2	0.55	2.60	0.48	**0.10**	5.0	1.29	0.13	0.13
3	0.55	2.60	0.48	**0.25**	5.0	3.23	0.18	0.31
4	0.55	2.60	0.48	**0.50**	5.0	6.45	0.29	0.48
5	0.55	2.60	**1.10**	0.25	5.0	1.33	0.02	0.06
6	0.55	**1.80**	0.48	0.25	5.0	1.42	0.04	0.13
7	0.55	2.60	0.48	0.10	**15.0**	3.89	0.22	0.35
8	**2.25**	2.60	0.48	0.02	5.0	0.40	0.04	0.04
9	2.25	2.60	0.48	**0.10**	5.0	2.02	0.15	0.23
10	2.25	2.60	0.48	**0.25**	5.0	5.06	0.34	0.46
11	2.25	2.60	0.48	**0.50**	5.0	10.1	0.55	0.65

Accuracy:

1. Both models predict the same trends in F_{ref} vs. turbulence parameters.
2. Reasonable match at low f_p (~0.1).
3. Multiscale model generally over-predicts F_{ref}.
4. Error grows with f_p. This is as expected from theory [1].

[1] Mishchenko. *EM scattering by particles and particle groups*. 2014.

Computational cost:

Each PETRA-M run: ~300GB RAM and ~25 CPU-hours.

Each multiscale run: ~1 minute on a laptop with 8GB available RAM.

Broadened wave-spectrum coupled to RTFP code

Fully non-inductive, low-density ($\bar{n}_e \approx 0.52{\times}10^{20}\mathrm{m}^{-3}$) L-mode discharge.

First-pass ray-trajectories

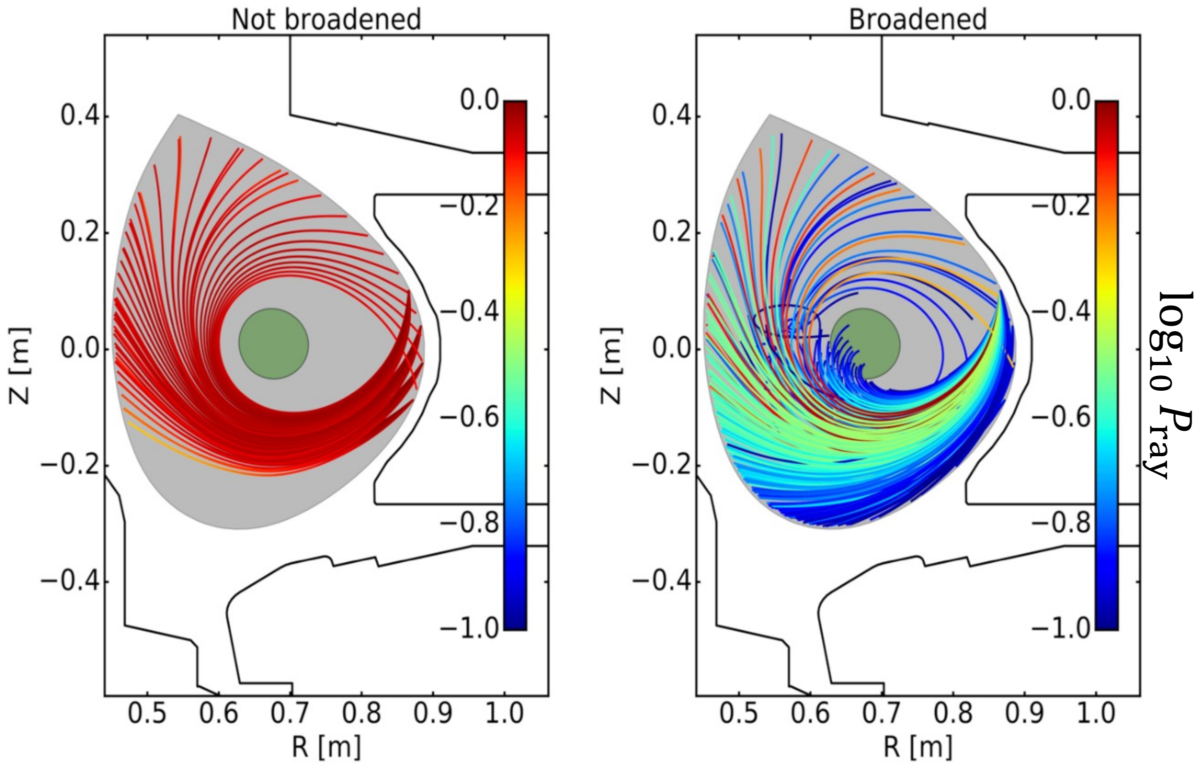

Modified wave-spectrum leads to increased on-axis damping on first-pass…

Simulated current profile

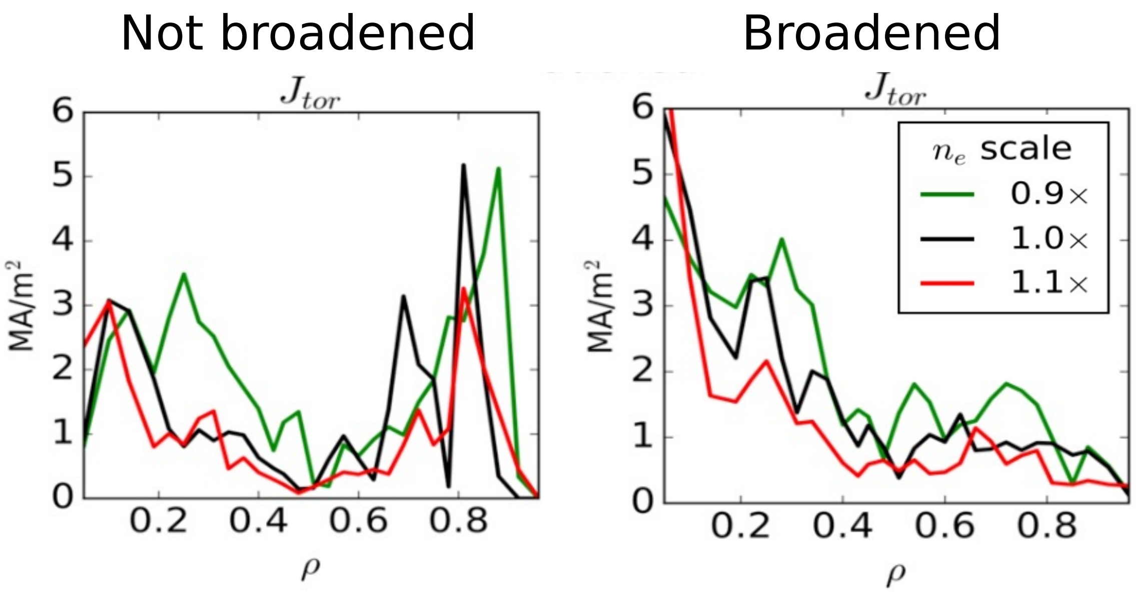

… and increase in on-axis current, decrease in off-axis peaks.

Solution scheme for general RTE

Generalise to arbitrary geometry:

- Account for scattering along the entire ray-trajectory.
- Varying SOL background and turbulence profiles.
- Mode-conversion between slow (S) and fast (F) mode.

Ray-trajectory and damping calculated in GENRAY/CQL3D

$$\boxed{\left(\frac{dP_j}{dt}\right)_r + 2\gamma(\mathbf{k}_j, \mathbf{r})P_j} = \boxed{\left(\frac{dP_j}{dt}\right)_{\mathrm{sct}}}$$

Stochastic kicks to ray-trajectory that rotate $\boldsymbol{k}_\perp$

$$\left(\frac{dP_j}{dt}\right)_{\mathrm{sct}} = \sum_{j'=S,F} - \boxed{\Sigma_{\mathrm{eff},j\to j'}(k_{||}, \mathbf{r})} |\mathbf{v}_{gr\perp}(\mathbf{k}_j, \mathbf{r})| P_j$$

$$+ \sum_{j'=S,F} \boxed{\Sigma_{\mathrm{eff},j'\to j}(k'_{||}, \mathbf{r})} |\mathbf{v}_{gr\perp}(\mathbf{k}_{j'}, \mathbf{r})| \int_{-\pi}^{\pi} \boxed{\hat{\sigma}_{\mathrm{eff},j'\to j}(\theta - \theta'; k_{||}, \mathbf{r})} P_{j'}(\theta', k_{||}, \mathbf{r}) d\theta'$$

Look-up tables in GENRAY

Prescribing scattering probabilities in a tokamak geometry

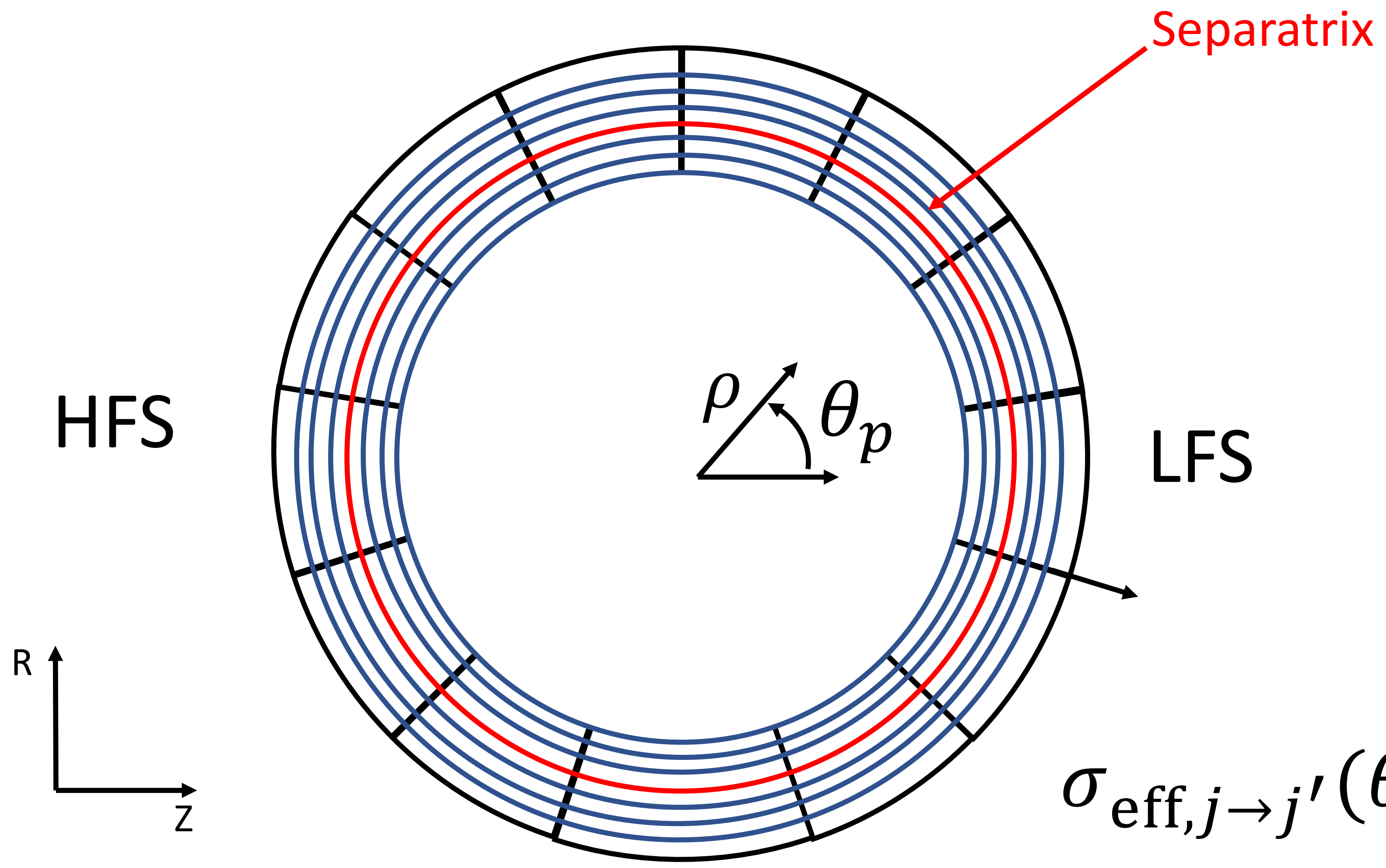

$$\sigma_{\mathrm{eff},j\to j'}(\theta;\rho,\theta_p,N_{||})$$

Radial (ρ) and poloidal (θ_p) tapering of filament PDFs in the SOL

LFS → HFS

Far SOL → Inside separatrix

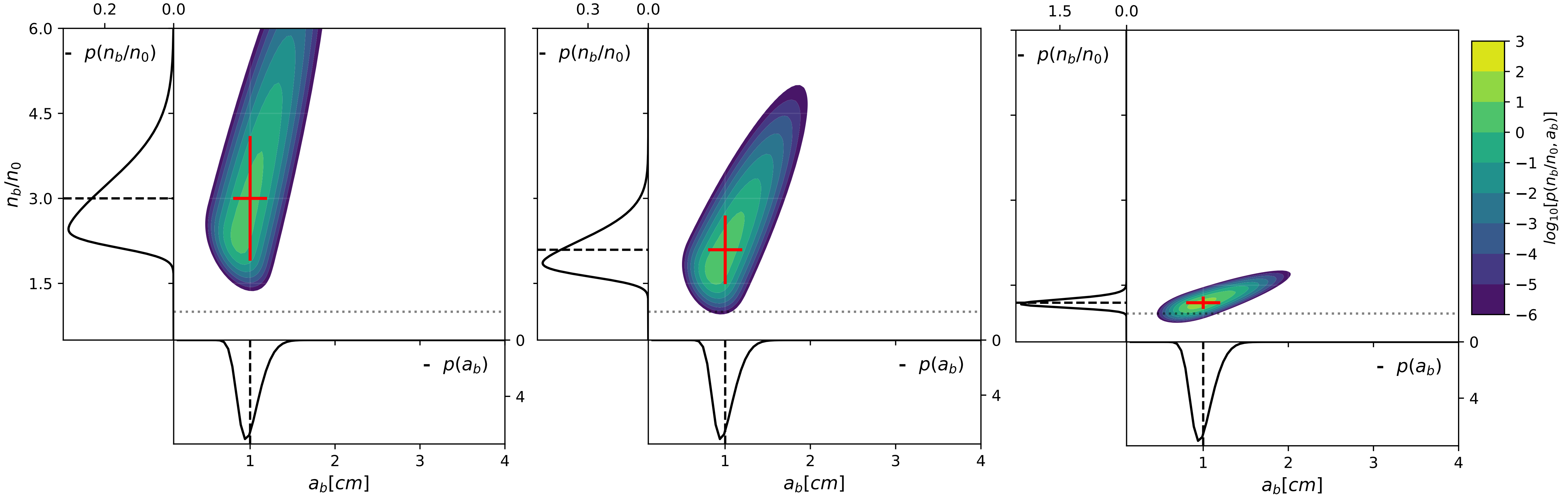

For more detail, see Biswas et al., NF. 2023.

Scattering is most prevalent in the far SOL at the outer mid-plane

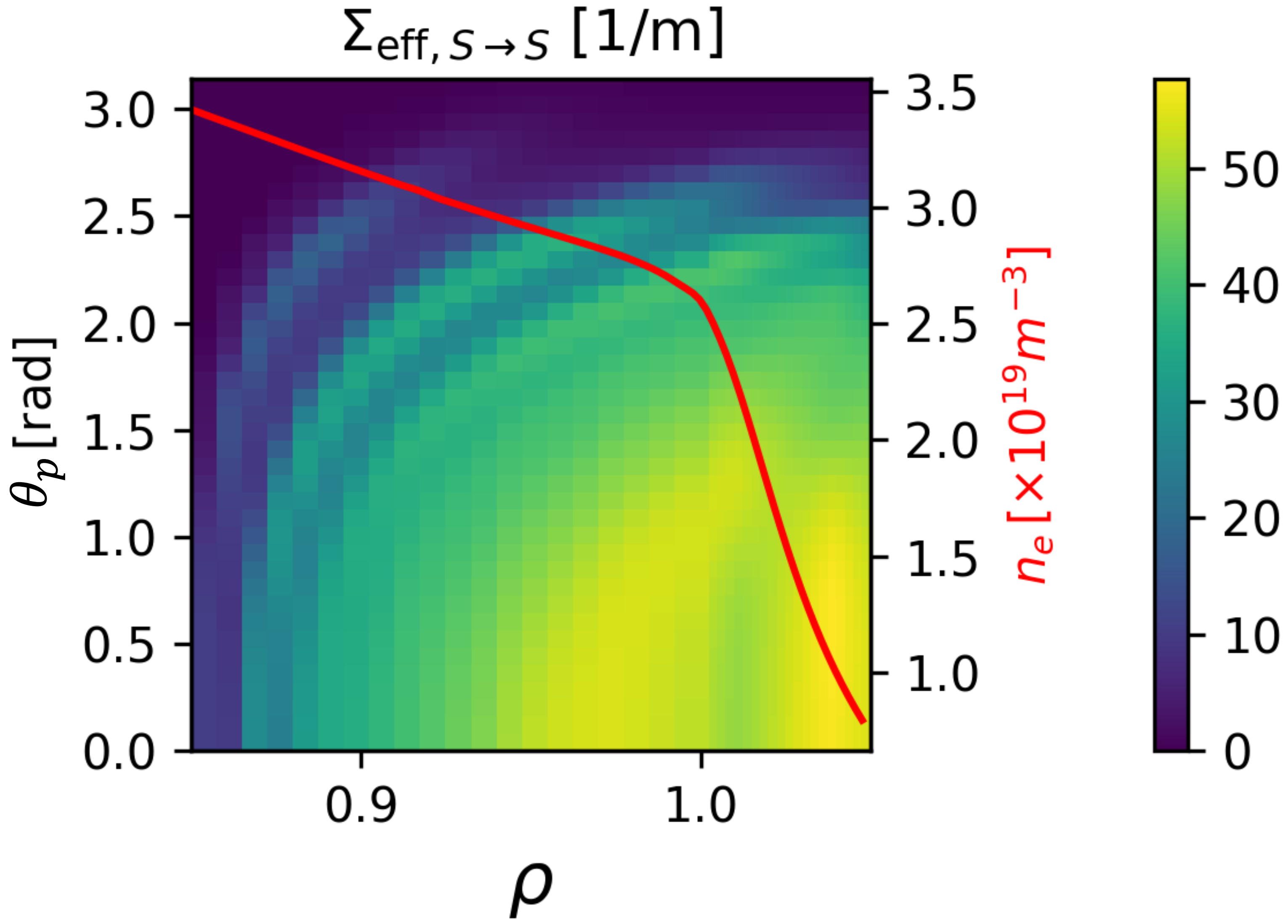

$N_{||} = 3$

Scattering is preferentially in outward direction

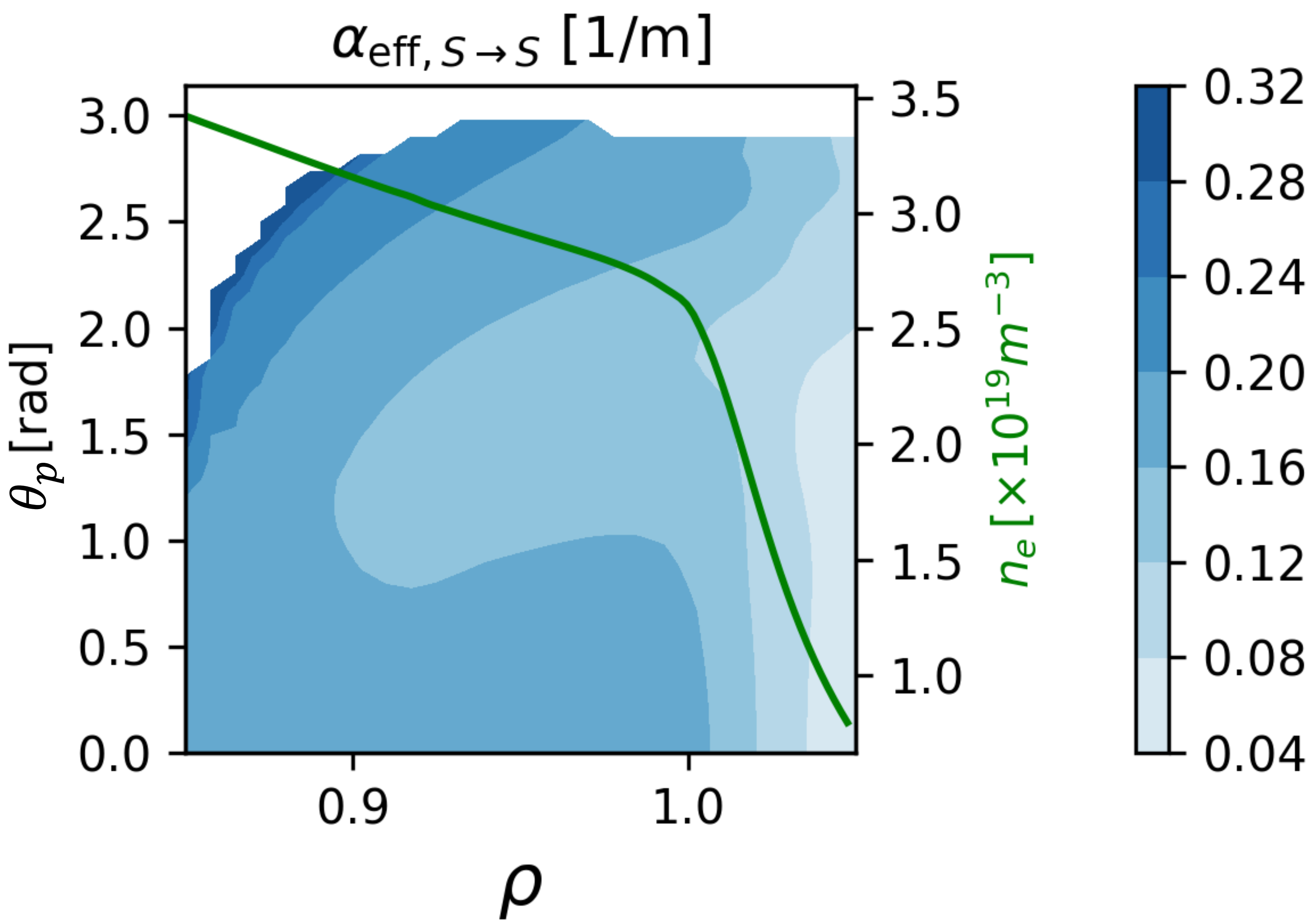

$N_{||} = 3$

Parametric scan of turbulence parameters

3D scan:

$\langle n_b/n_0 \rangle$: mean relative filament density (at LH antenna)

$\langle a_b \rangle$: mean filament radial width

f_p : packing fraction

Metric for agreement with experiment:

$$\bar{\chi}^2 = \frac{\sum_i (J_{\phi,\mathrm{sim}}(\rho_i) - J_{\phi,\mathrm{exp}}(\rho_i))^2}{\sum_i (J_{\phi,\mathrm{refsim}}(\rho_i) - J_{\phi,\mathrm{exp}}(\rho_i))}$$

Impact of scattering on LHCD saturates

$\bar{\chi}^2$ current density

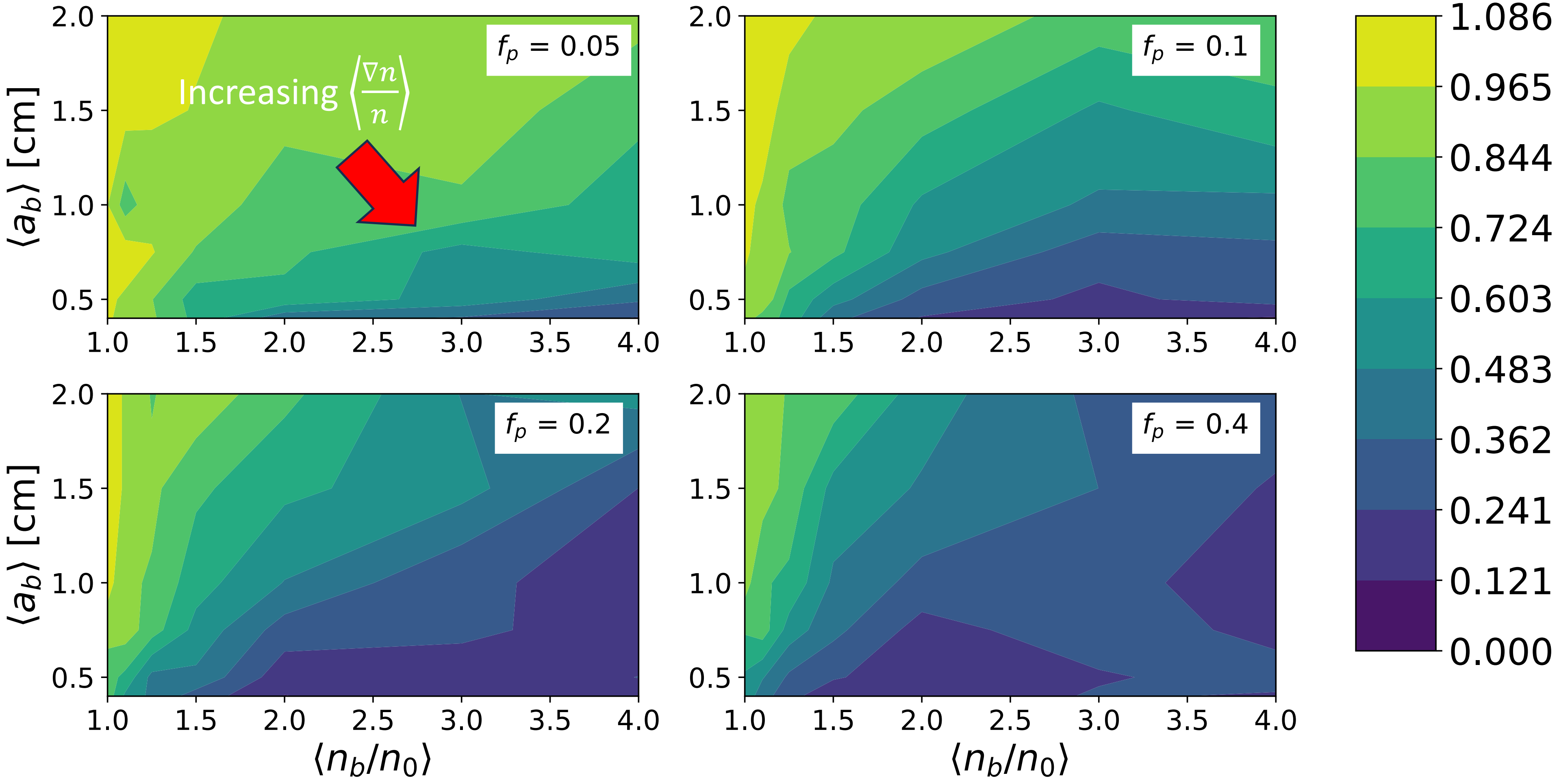

Impact of scattering on LHCD saturates

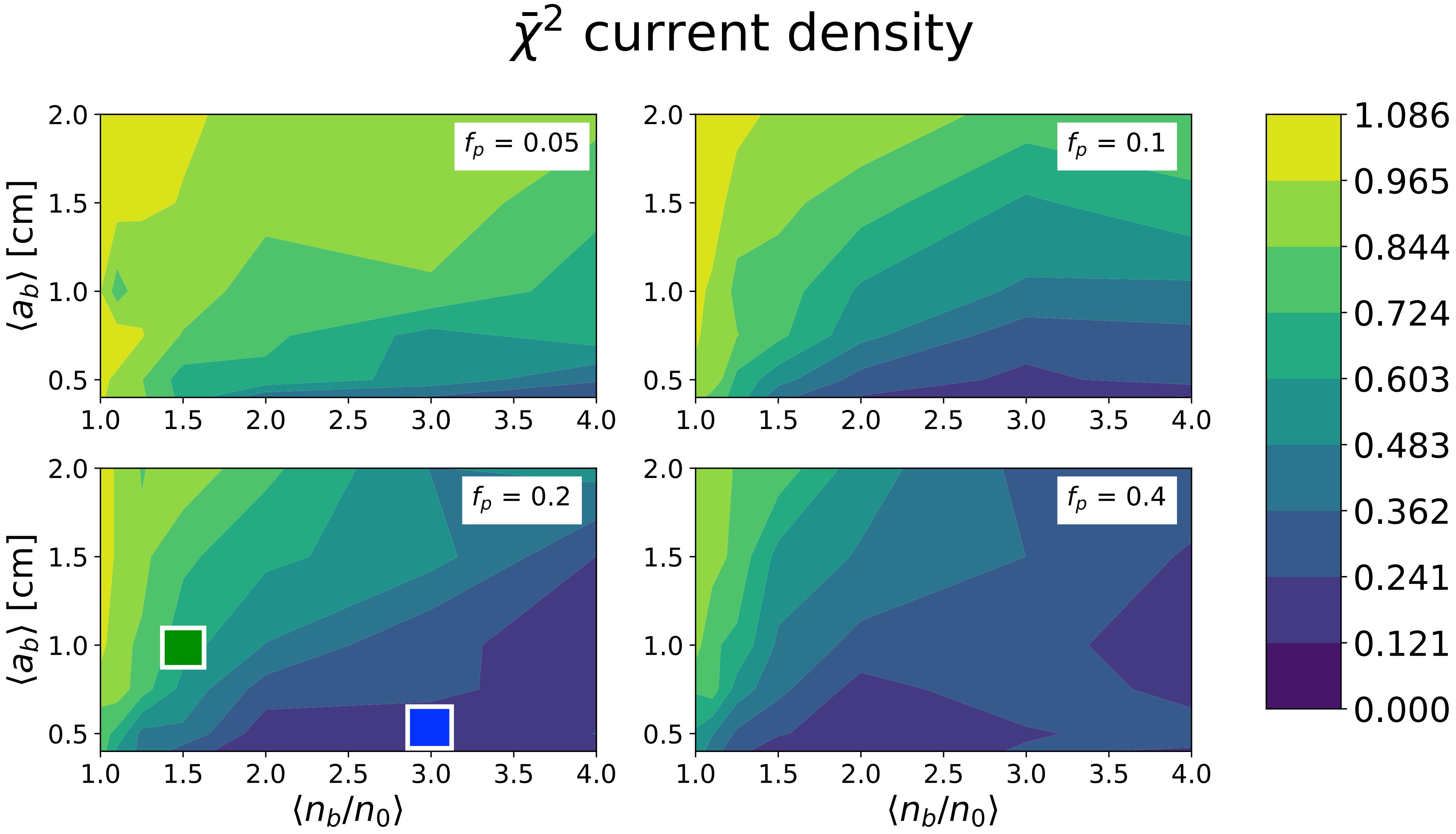

Saturated case finds good match to experiment

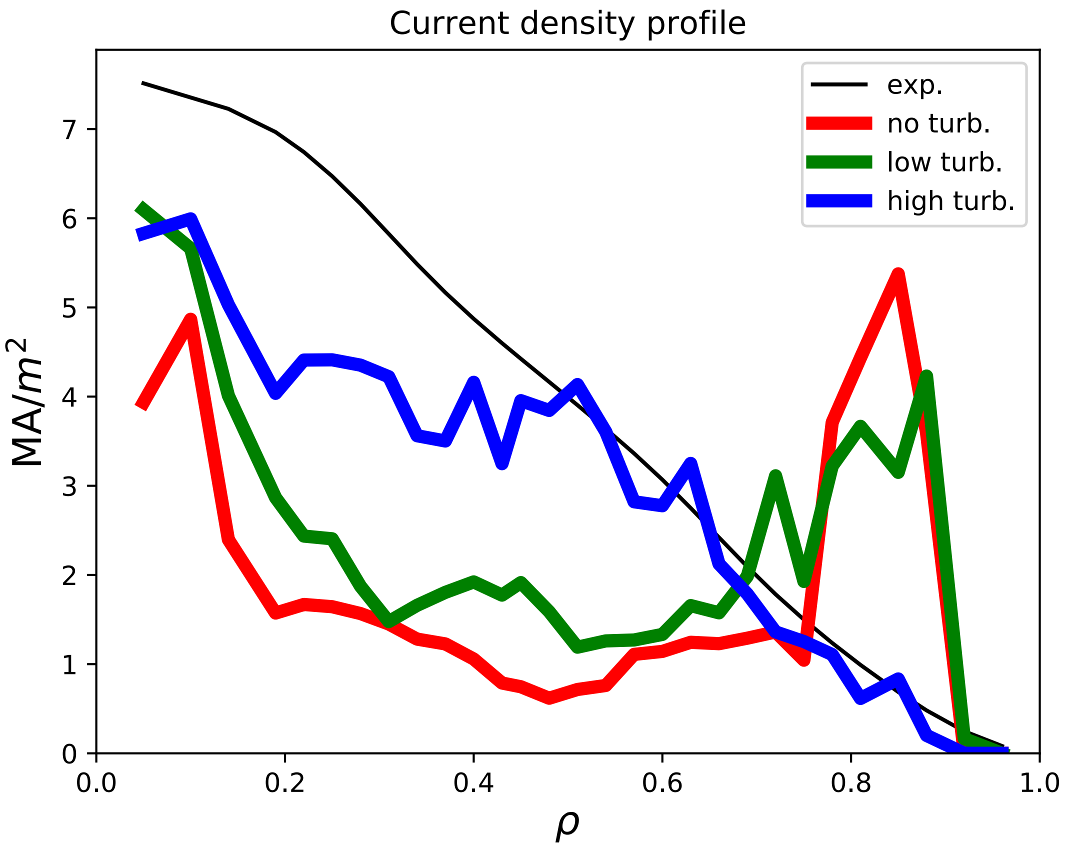

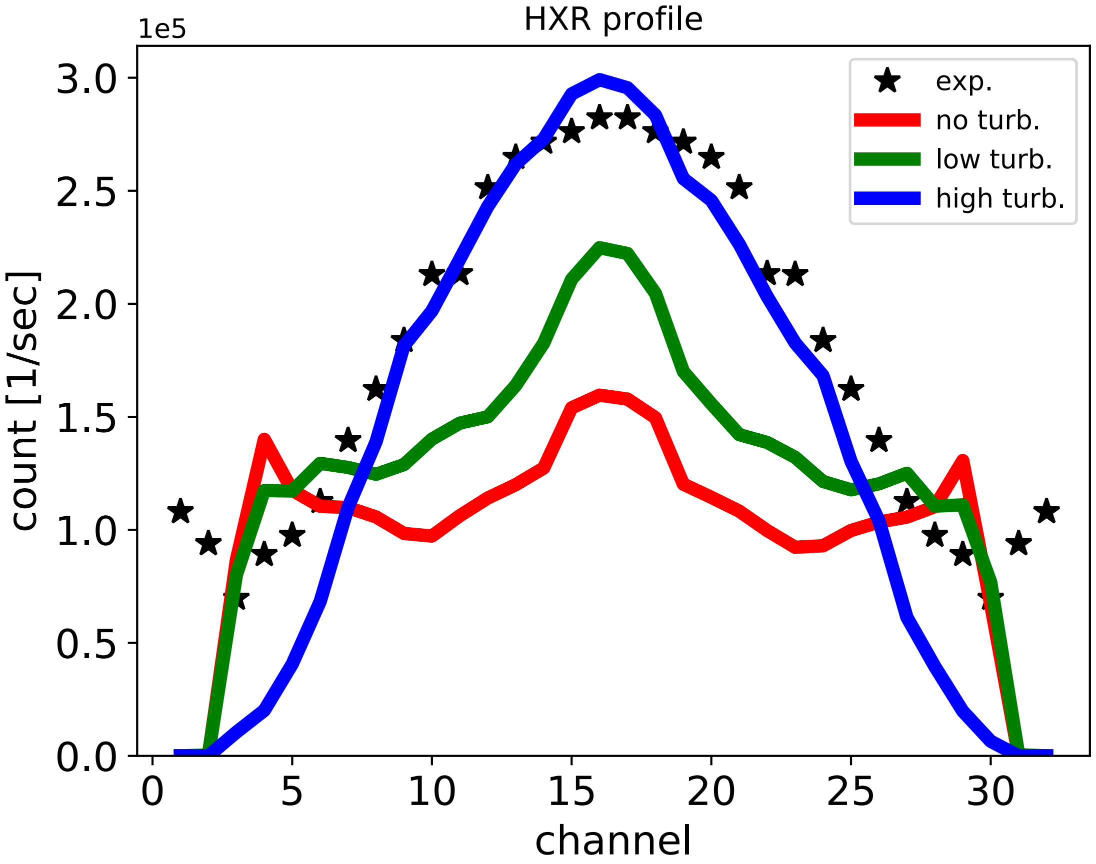

Scatter causes near-axis damping on first pass

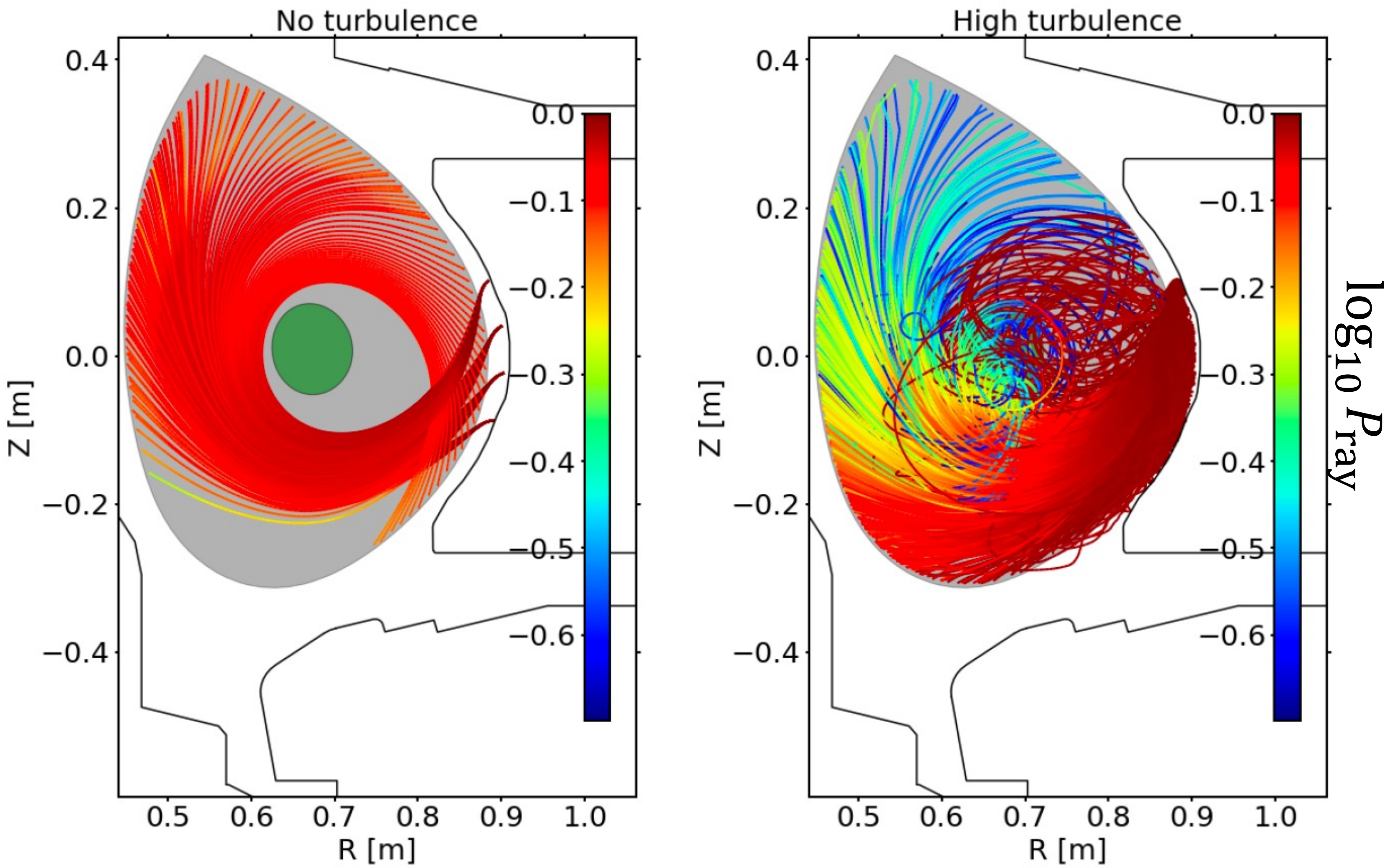

Simulating higher density discharges

$\bar{n}_e \approx 0.8{\times}10^{20}\mathrm{m}^{-3}$

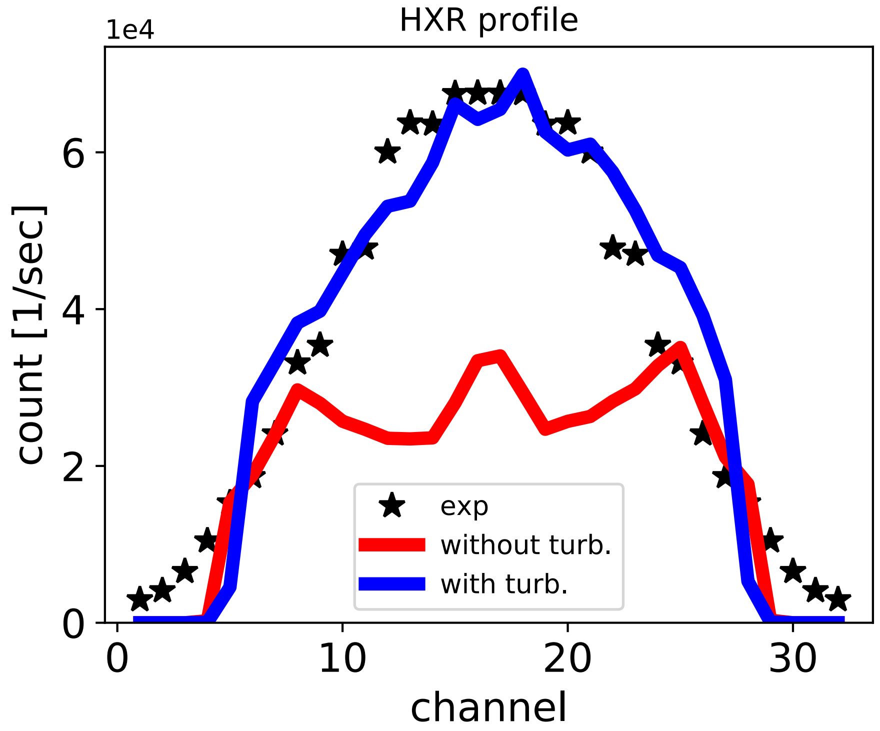

$\bar{n}_e \approx 1.1{\times}10^{20}\mathrm{m}^{-3}$

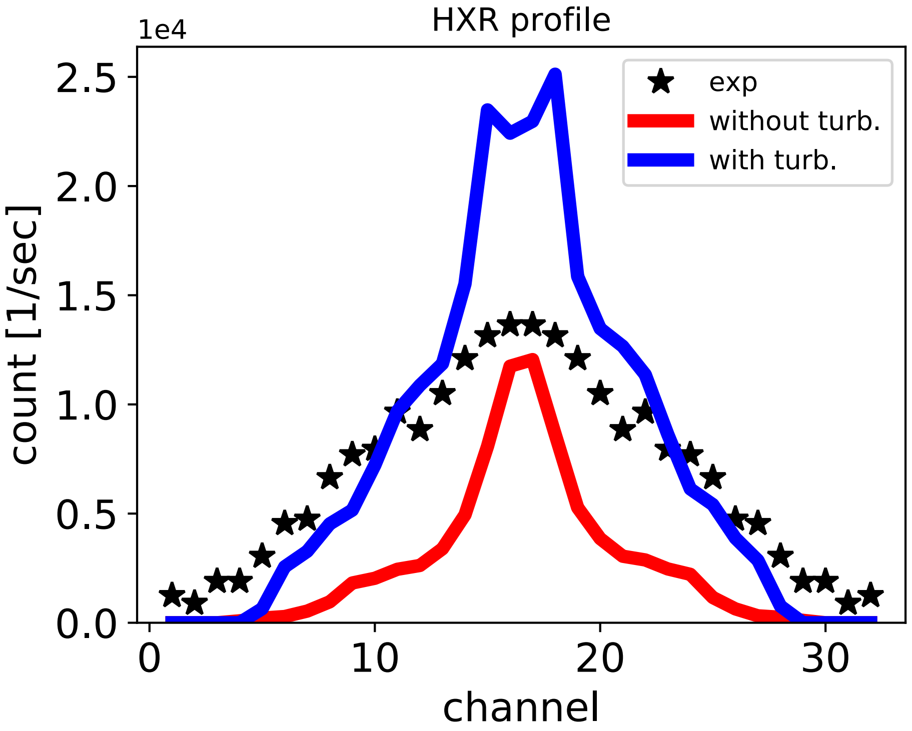

Caveat: not modeling DC electric field.

Saturation explained by filling in of phase-space

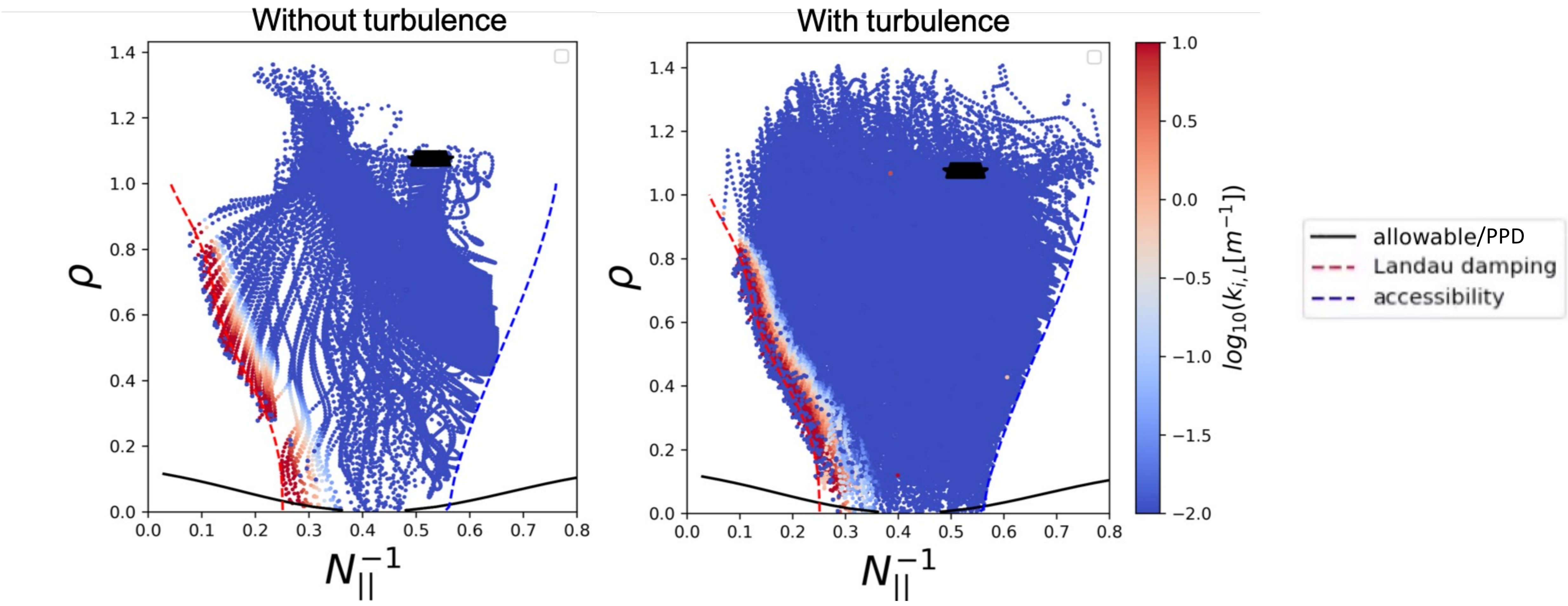

How important is asymmetric scatter?

Reversed scattering parity: $\sigma(\theta) \rightarrow \sigma(-\theta)$

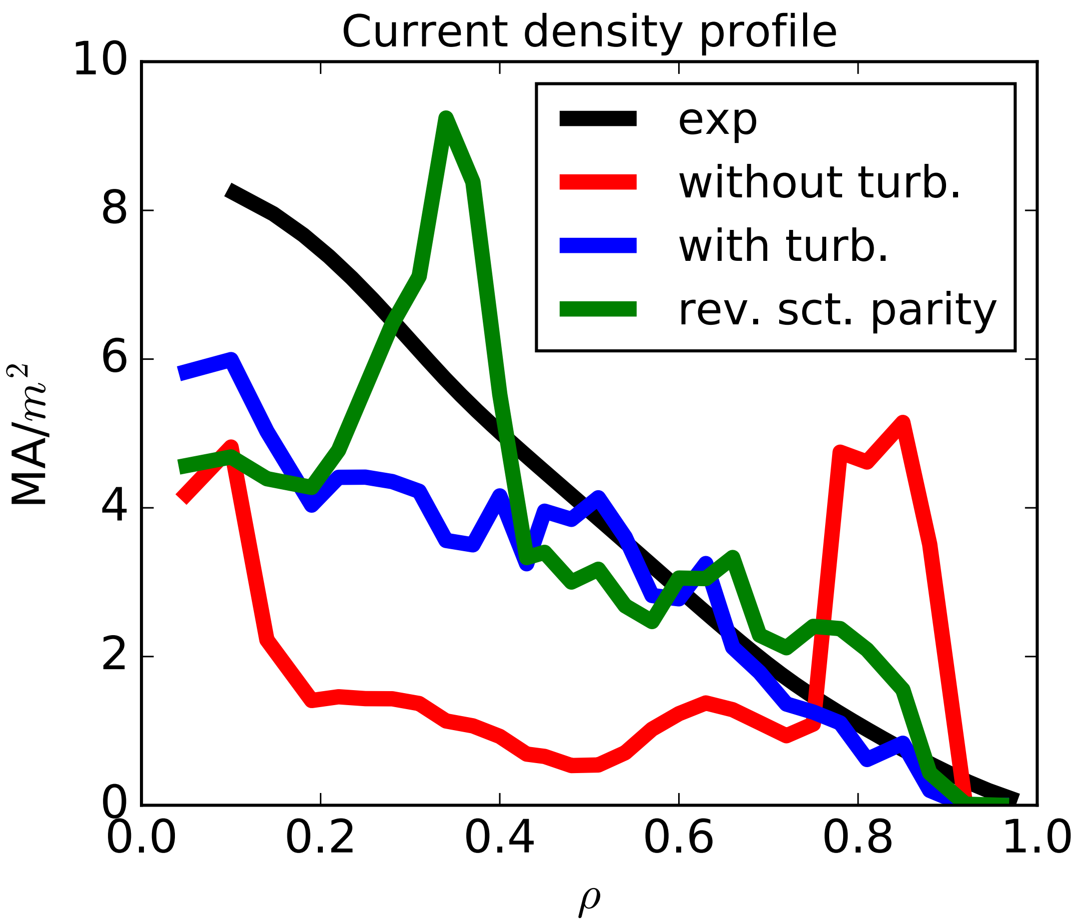

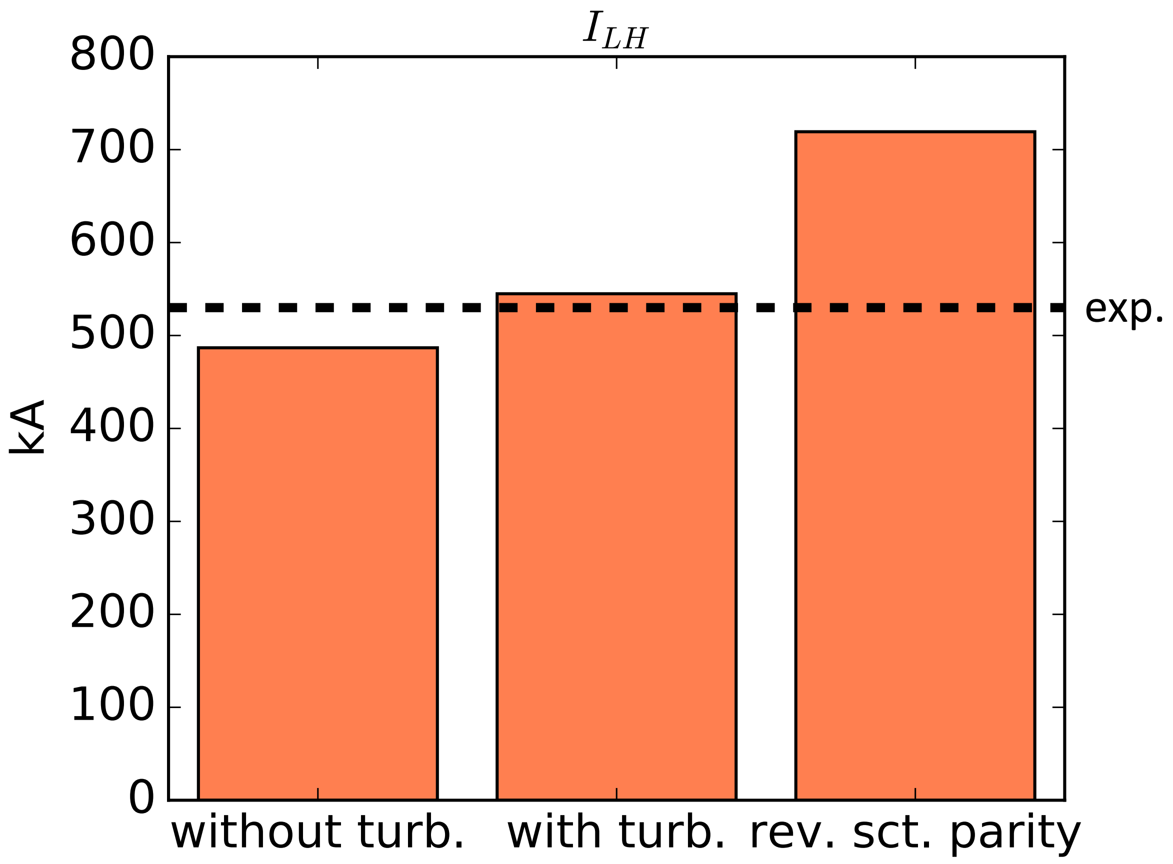

Conclusion

- For the first time, full-wave scattering effects on downstream damping and current drive modeled.
- Scattering can explain the spectral gap in Alcator C-Mod.
- Identified asymmetric scatter occurs, and is important.
- In C-Mod, effect of scattering is saturated. Exact filament PDF not important.

Mitigation strategies:

- Decrease SOL width/fluctuations
- HFS launch

Future work:

Can we directly measure RF scattering in the SOL?

Can scattering resolve *large* spectral gaps (e.g. WEST)?

Applications of ECCD. Impact on O-X mode conversion.

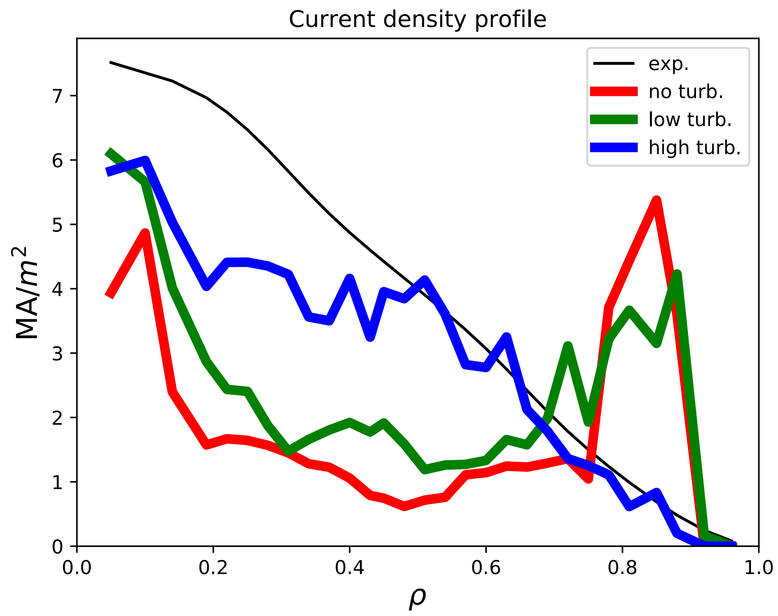

Future work: large spectral gap in WEST

Assuming toroidal mode-number conservation, LH waves cannot Landau damp in WEST.

But experiments show significant Landau damping in core…

Scattering breaks toroidal mode-number conservation. Is this strong enough to bridge the spectral gap?

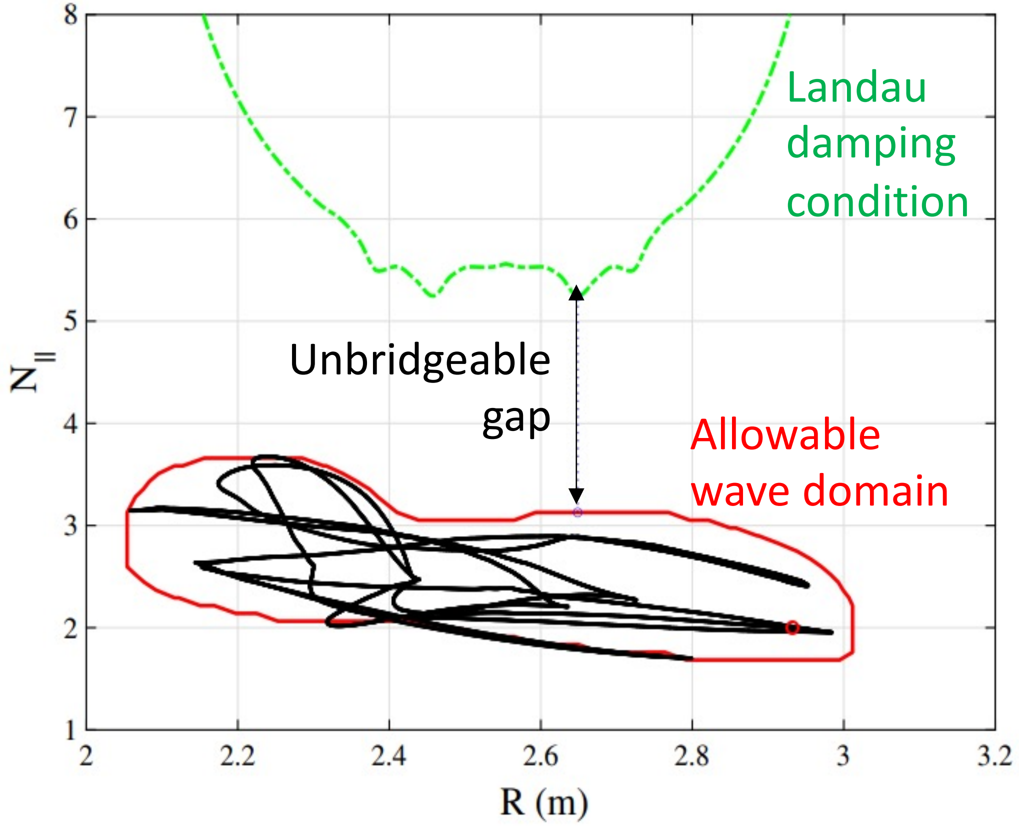

Peysson et al., Journal of Fusion Energy. 2020.

Lower hybrid current drive (LHCD)

Tokamaks require a steady-state source of current.

Lower hybrid (LH) waves ($\Omega_i^2 \ll \omega^2 \ll \Omega_e^2$) drive current by electron Landau damping.

$$N_{||} \equiv \frac{k_{||}c}{\omega} \gtrsim \frac{c}{3v_{te}}$$

Electrons preferentially accelerated in wave's parallel direction → asymmetric distribution function → net current

LHCD is sensitive to the phase-space trajectory of the wave

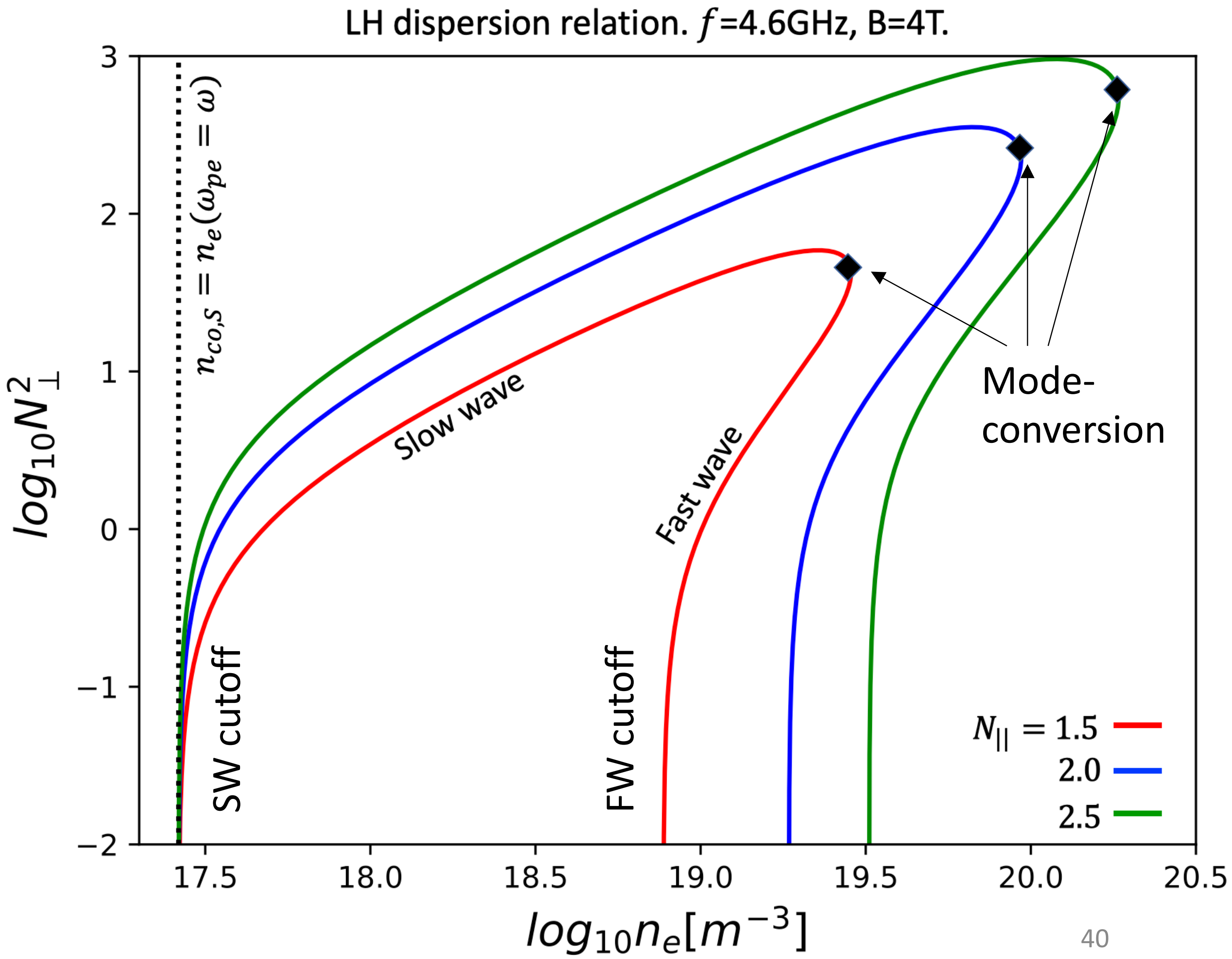

Fully non-inductive C-Mod discharge summary

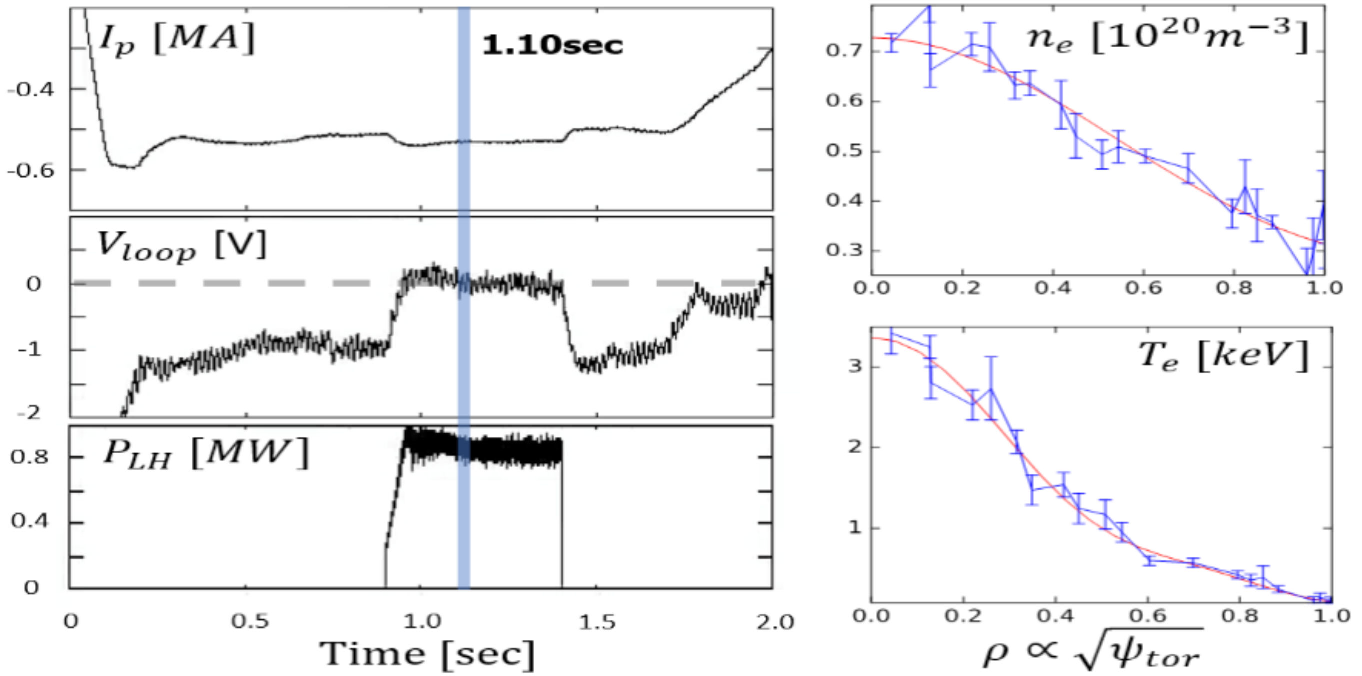

Figure 3.2: "Summary of Alcator C-Mod upper single-null L-Mode discharge #1101104011. $\overline{n_e} = 0.52 \times 10^{20}\,\mathrm{m}^{-3}$, $I_p = 530\,\mathrm{kA}$, and B=5.4 T. At t=1.10 sec, current is fully driven by 850 kW LH power launched at $N_{||} = -1.6$. Electron density (n_e) and temperature (T_e) profiles show experimental data from Thomson scattering (blue), and the fit profile (red) used in GENRAY/CQL3D runs."†

Ray-tracing equations

Cold plasma dispersion relation

$$D_0 = P_4 N_\perp^4 + P_2 N_\perp^2 + P_0 = 0$$

$$P_0 = \epsilon_{||} \left[\left(N_{||}^2 - \epsilon_\perp \right)^2 - \epsilon_{xy}^2 \right]$$

$$P_2 = \left(\epsilon_\perp + \epsilon_{||} \right) \left(N_{||}^2 - \epsilon_\perp \right) + \epsilon_{xy}^2$$

$$P_4 = \epsilon_\perp$$

Ray evolution in phase-space

$$\frac{d\mathbf{r}}{dt} = -\frac{\frac{\partial D_0}{\partial \mathbf{k}}}{\frac{\partial D_0}{\partial \omega}}$$

$$\frac{d\mathbf{k}}{dt} = \frac{\frac{\partial D_0}{\partial \mathbf{r}}}{\frac{\partial D_0}{\partial \omega}}$$

Ray damping in phase-space

$$\frac{dP}{dt} = -2\omega_I P$$

$$\omega_I = \frac{1}{(\partial D_0/\partial \omega)|_{\omega_r}} \sum_p D_I^{(p)}$$

Toroidal effects to ray trajectory

$$\frac{dm}{d\theta} = -\frac{\frac{\partial D_0}{\partial \theta}}{\frac{\partial D_0}{\partial m}} \approx -k_{||} R_0 q(r) \left(1 + \frac{\omega_{pe}^2/\Omega_e^2}{\epsilon_\perp}\right) \frac{(r/R_0)sin\theta}{1 + (r/R_0)cos\theta}$$

$$k_{||} = (\mathbf{k} \cdot \mathbf{B}/B) \approx \frac{m}{r}\frac{B_\theta}{B_\phi} + \frac{\mathbb{N}}{R}$$

Cold plasma dielectric tensor

$$\epsilon = \begin{bmatrix} \epsilon_\perp & -i\epsilon_{xy} & 0 \\ +i\epsilon_{xy} & \epsilon_\perp & 0 \\ 0 & 0 & \epsilon_{||} \end{bmatrix}$$

$$\epsilon_\perp = 1 - \sum_s \frac{\omega_{ps}^2}{\omega^2 - \Omega_s^2}$$

$$\epsilon_{xy} = \sum_s \frac{\Omega_s}{\omega} \frac{\omega_{ps}^2}{\omega^2 - \Omega_s^2}$$

$$\epsilon_{||} = 1 - \sum_s \frac{\omega_{ps}^2}{\omega^2}$$

Ray-tracing validity limit (1)

$$\mathbf{E} = \tilde{\mathbf{E}}(\mathbf{r}) e^{i(\mathbf{k}\cdot\mathbf{r} - \omega t)}$$

$$\boldsymbol{\nabla}\mathbf{E} = \left[i\left(\boldsymbol{\nabla} S\right) \tilde{\mathbf{E}} + \boldsymbol{\nabla}\tilde{\mathbf{E}} \right] e^{i(\mathbf{k}\cdot\mathbf{r} - \omega t)} \qquad \boldsymbol{\nabla} S = \mathbf{k}$$

$$\frac{c^2}{\omega^2}(\mathbf{k} - i\boldsymbol{\nabla}) \times [(\mathbf{k} - i\boldsymbol{\nabla}) \times \tilde{\mathbf{E}}] + \epsilon \cdot \tilde{\mathbf{E}} = \mathbf{D} \cdot \tilde{\mathbf{E}} = 0$$

If $\frac{|\boldsymbol{\nabla}\tilde{\mathbf{E}}|}{|\tilde{\mathbf{E}}|} \ll \mathbf{k}$ then ray-tracing valid.

$$\left(|\epsilon_{xy}| + N_{||}^2 \right) \frac{1}{k_\perp L} \ll 1$$

k-scattering model validity

$$1)\ \text{if}\ (k_\perp/\zeta_0)^2 \gg 1\ \text{then}\ (k_\perp/\zeta_0)^2 < \zeta_0 l_s$$

$$2)\ \text{if}\ k_\perp \lesssim \zeta_0\ \text{then}\ \zeta_0 l_s > 1$$

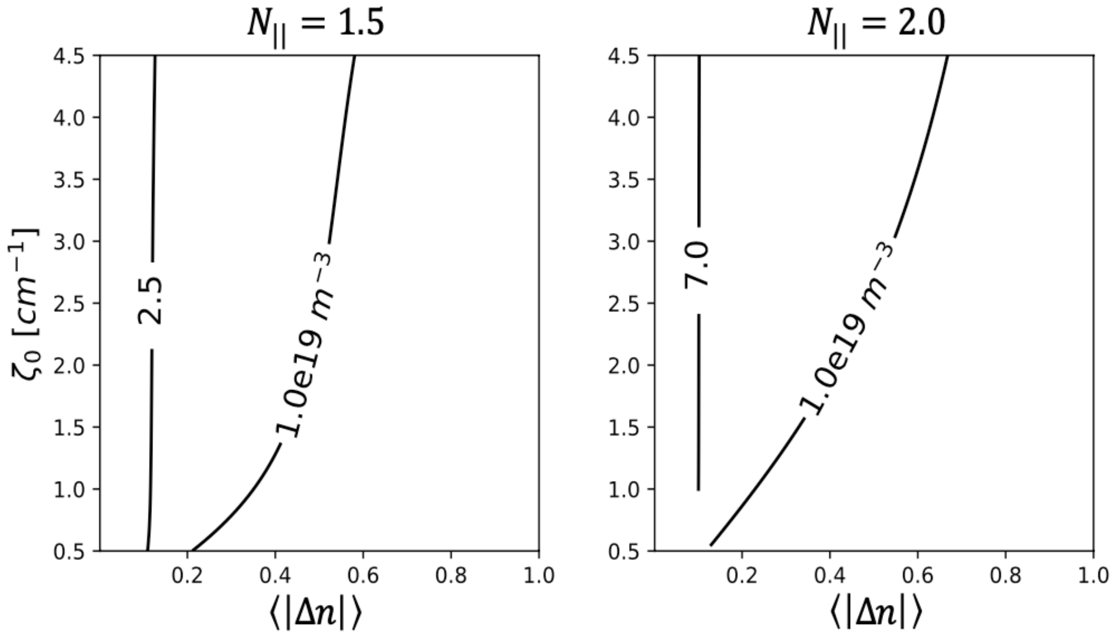

Ray trajectories on first-pass

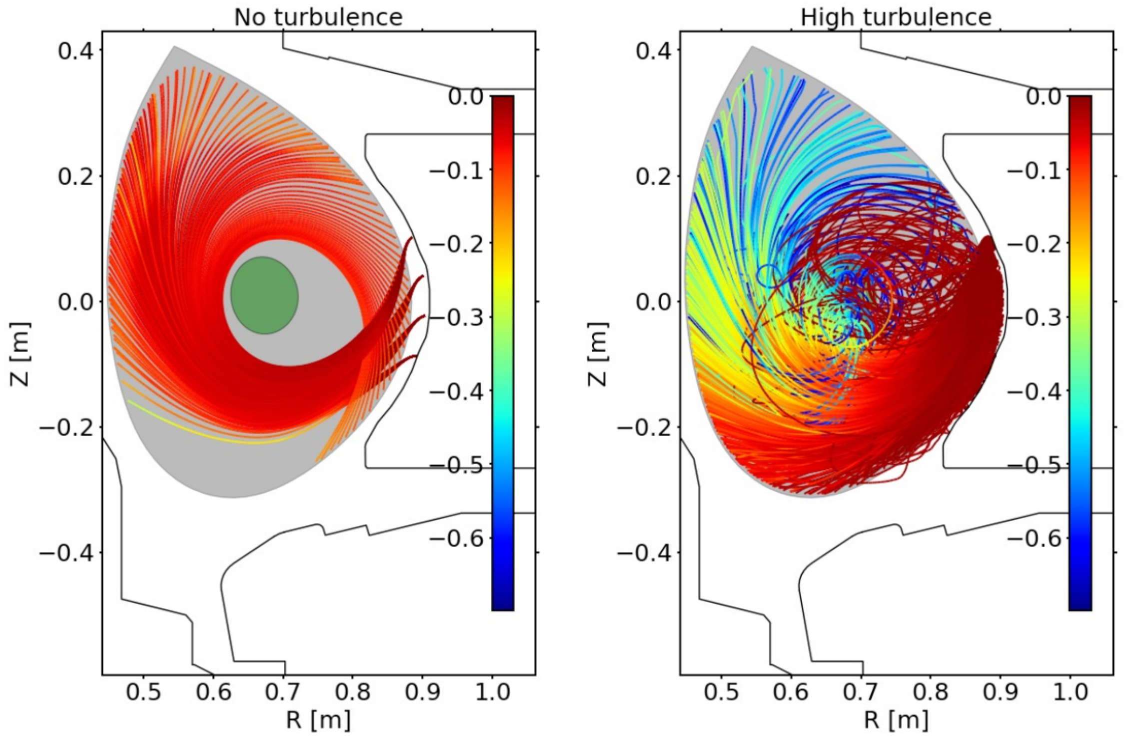

Figure 5.19: Ray-trajectories during first pass through the core. Plotting rays launched with $N_{||0} = 1.6 \pm 0.1$. Ray color denotes $\log_{10}$ of normalized ray power. Green patch denotes near-axis region ($\rho \leq 0.2$).

Sensitivity to choice of EFIT

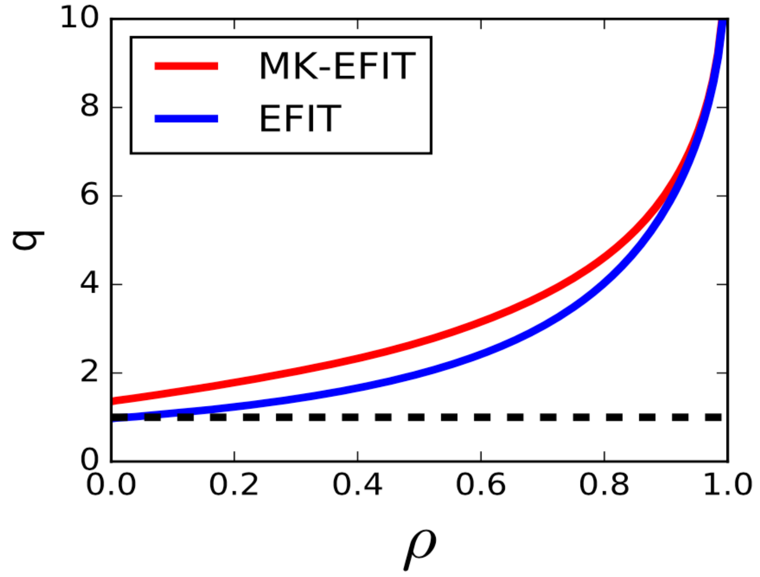

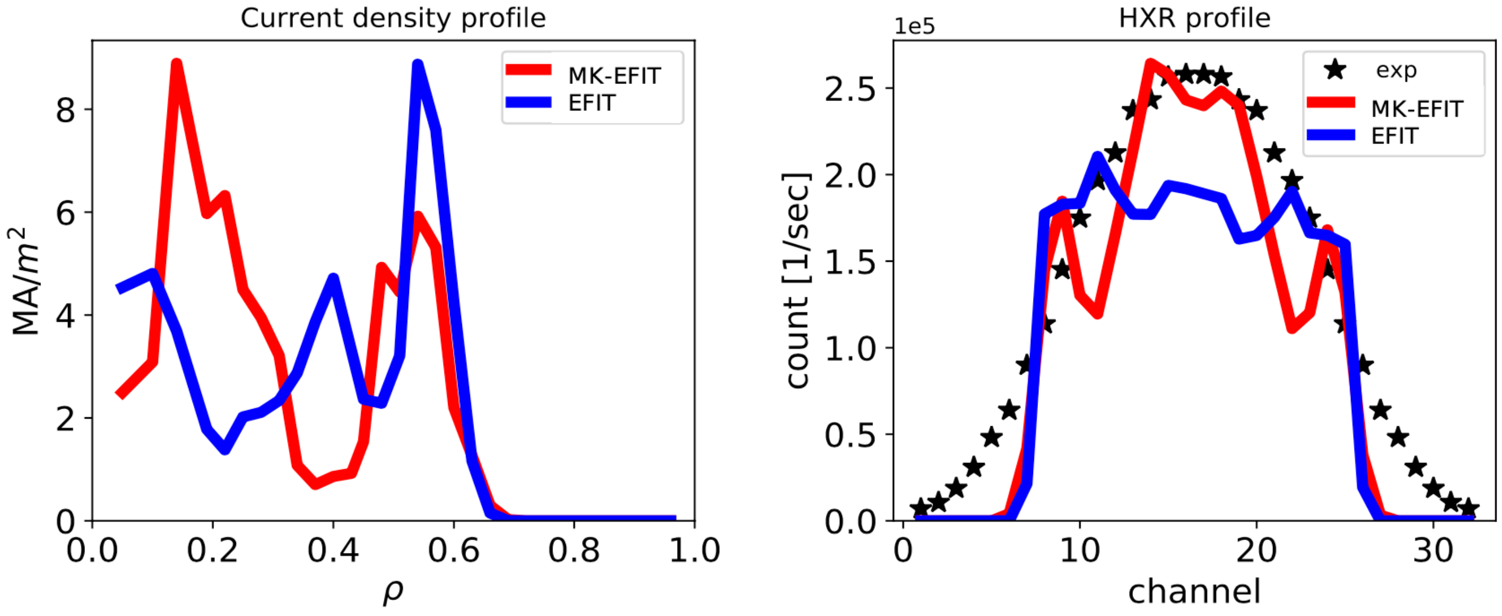

Figure 6.21: Sensitivity to equilibrium reconstruction model. Plotting simulated current (left) and HXR (right) profiles without scattering. C-Mod discharge #1120608016. Stars: experiment.

Impact of scattering on LHCD saturates

Equilibrium parameters
#1101104011
$t = 1.14s$
$\bar{n}_e \approx 0.52\times10^{20}\mathrm{m}^{-3}$
$T_{e0} \approx 3.5$ keV
$B = 5.4$ T
$I_p \approx 530$ kA

Launch parameters
$P_{LH} \approx 850$ kW
$N_{||0} = 1.6$

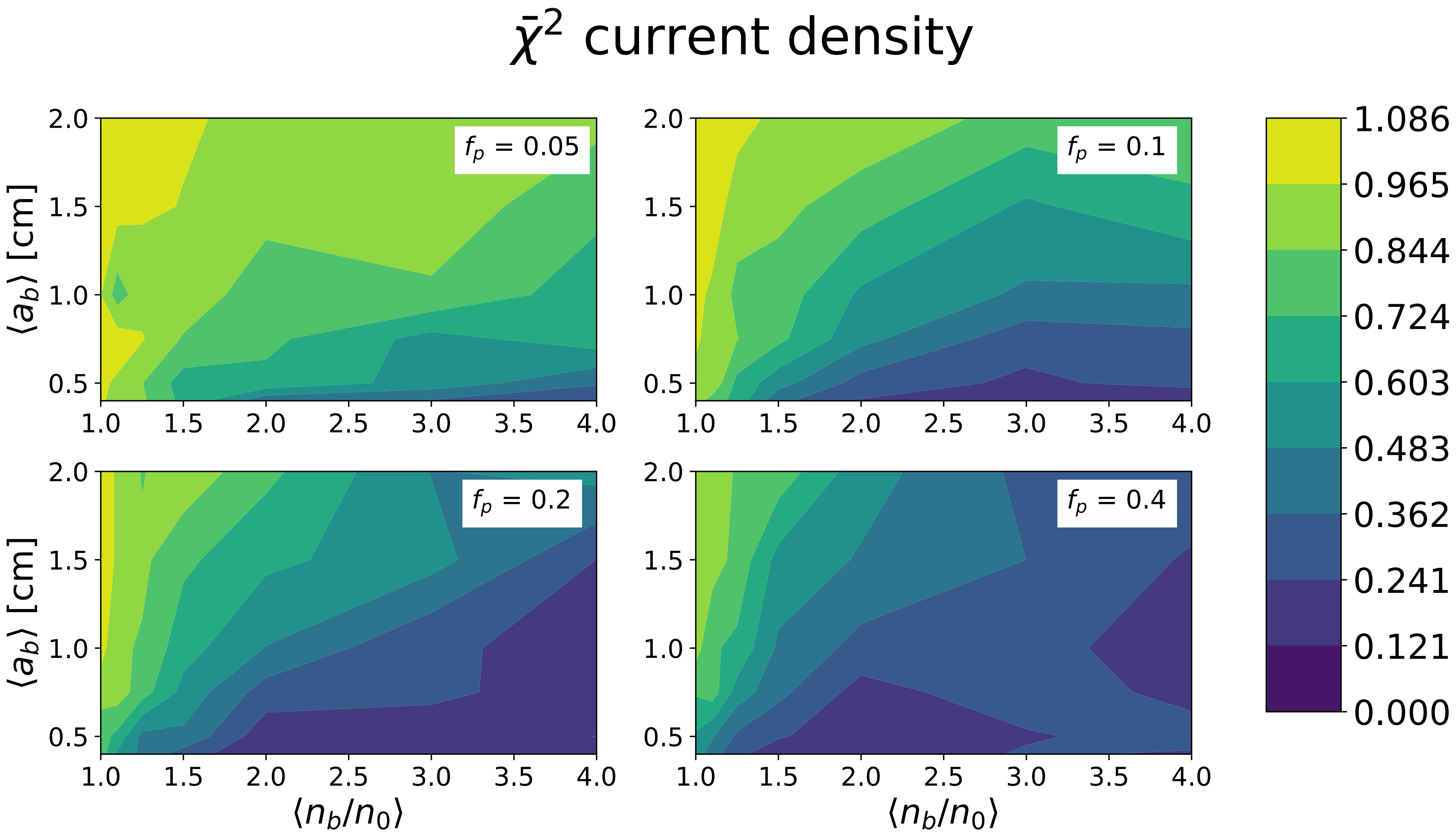

Initial rotation of ray-trajectory

$$\hat{\mathrm{b}} \cdot (\hat{e}_{\nabla\psi} \times \mathbf{k}_\perp) = k_\perp \sin\chi$$

$$k_\rho = k_\perp \cos\chi$$

$$k_\theta = k_{||}\frac{B_\theta}{B} - k_\perp \sin\chi \frac{B_\phi}{B}$$

$$k_\phi = k_{||}\frac{B_\phi}{B} + k_\perp \sin\chi \frac{B_\theta}{B}$$

$$\left|\frac{v_{gr,\rho}}{v_{gr,\theta}}\right| \approx \left|\frac{\epsilon_\perp k_\perp \cos\chi}{\epsilon_{||} k_{||}\frac{B_\theta}{B} - \epsilon_\perp k_\perp \sin\chi \frac{B_\phi}{B}}\right|$$

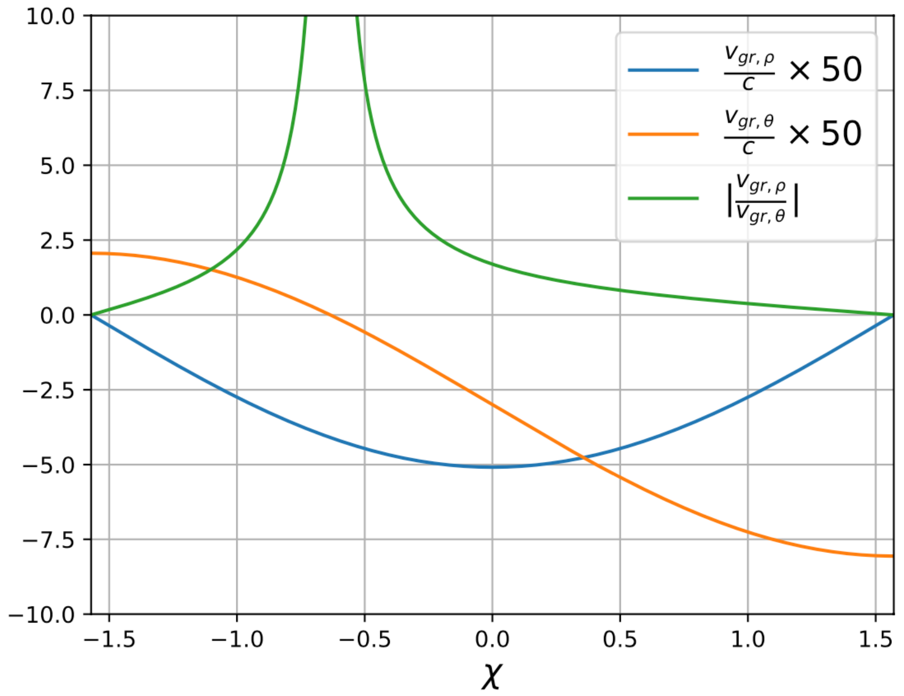

Figure 4.13: Initial ray orientation versus χ. For typical C-Mod launch parameters: $N_{||} = -1.6$, $B_\phi = -4\,\mathrm{T}$, $B_\theta = 0.4\,\mathrm{T}$, $n_e = 10^{19}\,\mathrm{m}^{-3}$.